Spring 2011

Quantum phase transitions in the presence of disorder and dissipation

Chetan Kotabage

Department: Physics

QUANTUM PHASE TRANSITIONS IN THE PRESENCE OF DISORDER AND DISSIPATION

by

CHETAN KOTABAGE

A DISSERTATION

Presented to the Faculty of the Graduate School of the

MISSOURI UNIVERSITY OF SCIENCE AND TECHNOLOGY

in Partial Fulfillment of the Requirements for the Degree

DOCTOR OF PHILOSOPHY

in

PHYSICS

2011

Thomas Vojta, Advisor
Paul E. Parris
Gerald Wilemski
Julia Medvedeva
Dirk Morr

ABSTRACT

A quantum phase transition is a phase transition at absolute zero occurring under variations in an external non-thermal parameter such as magnetic field or pressure. Quantum phase transitions are one among the important topics currently investigated in condensed matter physics. They are observed in various systems, e.g., in the ferromagnetic-paramagnetic phase transition in $LiHoF_4$ or in the superconductor-metal phase transition in nanowires.

A particular class of quantum phase transitions, which is phase transitions in the presence of disorder and dissipation, is investigated here. An example of this class is the ferromagnetic-paramagnetic phase transition in $Ni_{1-x}V_x$ or $CePd_{1-x}Rh_x$ caused by variations in chemical composition. In these system, disorder is due to random positions of doping element and the dynamics of order-parameter fluctuations is dissipative due to conduction electrons.

These quantum phase transitions are explained using the following approach: The Landau-Ginzberg-Wilson functional, which is derived from a microscopic Hamiltonian, is treated by the strong-disorder renormalization group method. For ohmic damping, phase transitions are strongly influenced by disorder and the critical point is an infinite-randomness fixed point, which is in the universality class same as that of the random transverse-field Ising model. The scaling form of observable quantities is activated type rather than conventional power-law type. For superohmic damping, the strong-disorder renormalization group method yields one of the recursion relationships different from ohmic damping. This difference indicates a more conventional transition for superohmic damping.

ACKNOWLEDGMENT

I am deeply grateful to Dr. Thomas Vojta for the support he gave during this work. I am greatly indebted to my advisory committee, Dr. Gerald Wilemski, Dr. Paul Parris, Dr. Julia Medvedeva, and Dr. Dirk Morr. I am very grateful to Dr. José A. Hoyos for his help. I thank the undergraduate and graduate students, who worked in Dr. Vojta's group during the completion of this work.

I thank the faculty members and the staff in the Physics department, the Curtis Law Wilson library, and the libraries in the Mobius cluster. I acknowledge the financial support of National Science Foundation, Research corporation, and Research board - University of Missouri. My sincere thanks to Jeanine Bruening for editing the thesis. I thank the Americal Physical Society, Dr. Thomas Vojta, Dr. Manuel Brando, and Dr. Philip Gegenwart for grating the permission to republish the figures, which were published in the journals of Americal Physical Society.

My stay in the US was not possible without the support of my family: my wife, Amita Naigaonkar, my parents, Vyankatesh Kotabage and Padmaja Kotabage, and my in-laws, Narhar Naigaonkar and Pratibha Naigaonkar. My sincere thanks to Pradnya Kulkarni, Digambar Kulkarni, and Deepa Kulkarni. This endeavor was not possible without the deep affection of many well-wishers, especially, Dr. Tejinder Walia, and Dr. Suhas Pethe.

TABLE OF CONTENTS

LIST OF ILLUSTRATIONS

LIST OF TABLES

1. INTRODUCTION

The phase change between ice and liquid water is a familiar example of a phase transition. Phase transitions occur in many diverse systems. Because they are complex phenomena, formulation of a theoretical framework to explain them has been a challenge for many decades. The tools of statistical mechanics have been used to understand these many-body phenomena.

A quantum phase transition is a special kind of phase transition observed at absolute zero due to variations in a nonthermal parameter such as pressure or magnetic field. This chapter explains the basics of phase transitions[1] generally and quantum phase transitions in particular.

1.1. THE BASICS OF PHASE TRANSITIONS

Variations in energy configurations of the constituents of a substance can qualitatively change the physical properties[2] of that substance. The phases are these energy configurations, which often correspond to various symmetries, and the changes in these configurations are phase transitions. Figure 1.1 shows the phases of a typical fluid substance as a function of pressure and temperature. The solid lines represent the boundaries between phases. The liquid-gas phase boundary ends at the critical point C. A phase transition takes place when the system crosses the phase boundary due to variations in the external parameters. Crossing of the phase boundary is accompanied by singularities in the physical properties of the substance.

In general, phase transitions are classified as either *first-order* or *continuous* (or *second-order*). In a first-order phase transition, both phases coexist at the phase boundary. The phase change is accompanied by latent heat[3], which is evidence of abrupt structural changes in the substance. The first derivative of the free energy with respect to a state variable is discontinuous in a first-order phase transition.

---

[1]For more details see, e.g., [1, 2, 3].

[2]These include, e.g., mechanical, electrical, or magnetic characteristics.

[3]Latent heat is the heat absorbed by a substance at a constant temperature as it changes from one phase to another.

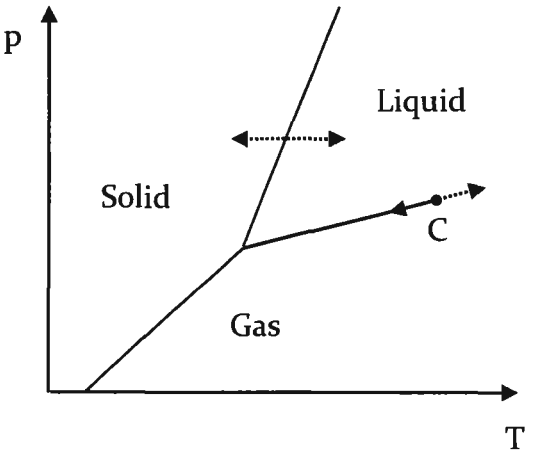

Figure 1.1. Phase diagram of a typical fluid substance as a function of pressure, p, and temperature, T. Point C denotes the critical point. The dotted arrow across the solid and the liquid phase shows a first-order phase transition. The dotted arrow passing through the critical point shows a continuous phase transition.

The dotted arrow drawn across the solid-liquid phase boundary in figure 1.1 is an example of a first-order phase transition. It corresponds to the example mentioned above of ice and liquid water.

The dotted arrow passing through the critical point C in figure 1.1 shows an example of a continuous phase transition. The two phases (i.e., liquid and gas) that coexist on the phase boundary become indistinguishable at that point. In such a transition, the free energy and its first derivative with respect to a state variable are continuous, and there is no latent heat involved. The ferromagnetic-paramagnetic phase transition in iron at 1043°K is another example of a continuous phase transition.

A continuous phase transition is generally characterized by an order parameter 'ϕ', which is a physical quantity that is zero on one side of the critical point and non-zero on the other. For example, the order parameter of the liquid-gas transition in figure 1.1 can be the difference between liquid and gas densities. Defining the order parameter for a phase transition can be difficult.

The spatial and temporal fluctuations of the order parameter are important in addition to the average of order parameter. These are quantified by a two-point

correlation function[4] :

$$C(\mathbf{x},\tau) \equiv \langle \phi(0,0) \cdot \phi(\mathbf{x},\tau) \rangle - |\langle \phi \rangle|^2 \ . \tag{1}$$

One way to obtain experimental information about a continuous phase transition is by means of scattering experiments[5]. The scattering cross-section of probing particles is proportional to the Fourier transform of the two-point correlation function. As a system approaches the critical point, order-parameter fluctuations grow in space and time. These are correlated up to a length called the correlation length[6], ξ; likewise, the typical time scale of order-parameter fluctuations is defined as correlation time, τ_c. The length and time scales of order-parameter fluctuations become large at the critical point. An example is the critical point of CO_2 at 304°K and 73 atm pressure. The transparent CO_2 turns milky as it approaches the critical point. The increasing length scale of density (i.e., the order parameter) fluctuations eventually becomes comparable to the wavelength of visible light; consequently, the light is scattered. This phenomenon is known as critical opalescence [5].

Empirical studies[7] of systems approaching a continuous phase transition at a temperature T_c indicate power-law relationships between observable quantities. Specifically, the correlation length ξ diverges as $|r|^{-\nu}$, where r is the reduced temperature ($r = (T - T_c)/T_c$) and ν is the correlation-length critical exponent. Likewise, the correlation time diverges as

$$\tau_c \sim |r|^{-\nu z} \ , \tag{2}$$

where z is the dynamical critical exponent. These and other power laws of observable quantities (Table 1.1) can be theoretically derived from the scaling hypothesis.

[4]The notation $\langle a \rangle$ represents the thermal average of a. The thermal average of a quantity is the average at a constant temperature in an equilibrium state.

[5]For example, see [4].

[6]The relationship between the two-point correlation function and the correlation length (i.e., equation (10)) is addressed in section 1.2 below.

[7]For instance, see [6, 7, 8, 9].

1.2. THE SCALING HYPOTHESIS

The following discussion of the scaling hypothesis considers a magnetic system that undergoes a ferromagnetic-paramagnetic continuous phase transition. Thermodynamic quantities at the critical point can be derived from the free energy density, which is given by

$$f = -\left(\frac{k_B T}{V}\right) \ln Z \,, \tag{3}$$

where V is volume, k_B is a Boltzmann constant, T is the temperature, and Z is the canonical partition function. An example is the magnetic susceptibility χ in the absence of an external field h :

$$\chi = -\left(\frac{\partial^2 f}{\partial h^2}\right)_{h=0} \,, \tag{4}$$

or the magnetization in the absence of an external field

$$m = \left(-\frac{\partial f}{\partial h}\right)_{h=0} \,. \tag{5}$$

Widom propounded the scaling hypothesis on a phenomenological basis [10]. The hypothesis states that the free energy density of a system sufficiently close to the critical point has a so-called scaling form

$$f(r,h) = |r|^{1/y}\, \psi_{\pm}(h\,|r|^{-(x/y)}) \,, \tag{6}$$

where the scaling function ψ is a function of only one variable.

The scaling function differs for $r > 0$ (i.e., ψ_+) and $r < 0$ (i.e., ψ_-). Widom found that the values[8] of x and y can be chosen such that the functions $\psi_\pm$ are identical for apparently dissimilar systems. The scaling hypothesis has played an important role in the development of the renormalization group[9] [11].

[8]Here, x and y are real numbers.

[9]The renormalization is the modern theory of critical phenomena. Using the renormalization group, the scaling form of the free energy can be derived from first principles.

Use of the free energy density in equation (6) to calculate the magnetic susceptibility of equation (4) yields the power law

$$\chi = |r|^{(1-2x)/y} \frac{\partial^2 \psi_{\pm}(0)}{\partial h^2} . \tag{7}$$

If this result is compared with experimental observations at the critical point, where the susceptibility diverges as $|r|^{-\gamma}$ (see table 1.1), then the susceptibility critical exponent can be written as $\gamma = \frac{2x-1}{y}$. In general, a critical exponent describes the nonanalytic behavior of an observable quantity near the critical point. The critical behavior of a phase transition is described by a collection of appropriate critical exponents, which depend on the dimension of the system and the order-parameter, and on the symmetry of the Hamiltonian. Table 1.1 lists the critical exponents of a magnetic transition and their defining conditions. Dissimilar systems of equal dimensions that are characterized by order parameters of the same dimensions have identical critical exponents. This phenomenon is called *universality*, which shows that although microscopic details may be responsible for various phases in a system, they do not control its critical behavior.

The critical exponents α, β, and δ can be expressed in terms of x and y by taking a partial derivative of the free energy density (i.e., equation (6)) with respect to a suitable variable. Since the scaling form of the free energy density contains only two exponents (i.e., x and y), it leads to different relations among the critical exponents.

Table 1.1. Definitions of the critical exponents in a magnetic phase transition: r is the reduced temperature, d is the system's dimension, $|\mathbf{x}|$ is a spatial distance, and h is the external magnetic field.

Critical exponent	Definition	Condition
ν	Correlation length $\xi \propto \lvert r\rvert^{-\nu}$	$r \to 0$; $h = 0$
η	Correlation function $C(\mathbf{x}) \propto \lvert\mathbf{x}\rvert^{-d+2-\eta}$	$r = 0$; $h = 0$
γ	Susceptibility $\chi \propto \lvert r\rvert^{-\gamma}$	$r \to 0$; $h = 0$
α	Specific heat $c \propto \lvert r\rvert^{-\alpha}$	$r \to 0$; $h = 0$
β	Order parameter $\langle\phi\rangle \propto (-r)^{\beta}$	$r \to -0$; $h = 0$
δ	Critical isotherm $h \propto \langle\phi\rangle^{\delta}$	$r = 0$; $h \to 0$

These so-called scaling laws are

$$\alpha + 2\beta + \gamma = 2 \tag{8}$$

and

$$\alpha + \beta(\delta + 1) = 2 \, . \tag{9}$$

The scaling hypothesis of the equal-time two-point correlation function provides a basis for further discussion of the scaling law :

$$C(\mathbf{x}) = \frac{\vartheta_{\pm}(|\mathbf{x}|/|r|^{-\nu})}{|\mathbf{x}|^{d-2+\eta}} \, , \tag{10}$$

where ν is the correlation-length critical exponent, $|\mathbf{x}|$ is a distance, d is the dimension, and η is the correlation-function critical exponent. The theory of linear response,[10] which relates the magnetic susceptibility to the two-point correlation function, gives the scaling law

$$(2 - \eta)\nu = \gamma \, . \tag{11}$$

The singular part of the free energy density is proportional to ξ^{-d} since the correlation length is the only useful length at the critical point. This relation gives the hyperscaling law

$$\nu d = 2 - \alpha \, , \tag{12}$$

which involves the dimension. The hyperscaling law holds below a specific dimension called the *upper critical dimension*[11].

1.3. QUANTUM PHASE TRANSITIONS

Quantum phase transitions are zero-temperature phase transitions that occur under variations in an external nonthermal parameter [15, 16, 17]. A quantum phase

[10] See, e.g., [4, 12].

[11] Discussed below in section 2.1. More details can be found in [13, 14].

transition can be a first-order or a continuous phase transition. A phase transition in which the two distinct degenerate ground states coexist is called a *first-order quantum phase transition.*

A continuous quantum phase transition has no special degeneracy as in $LiHoF_4$. The phase diagram of this substance as a function of temperature and external magnetic field is shown in figure 1.2 [18]. The ferromagnetic-paramagnetic phase transition can occur in two ways: by increasing the temperature at a small external field, as shown by the solid arrow, or by increasing the external field at a low temperature, as shown by the dotted arrow. The dotted arrow shows a continuous quantum phase transition due to quantum fluctuations, which arise from Heisenberg's uncertainty principle. As the external field increases, quantum fluctuations also increase and compete with the order in the ferromagnetic phase. They destroy it beyond the critical point, which results in the paramagnetic phase.

Since quantum phase transitions occur exactly at absolute zero, they cannot be attained in experiments; nevertheless, the effects of a quantum critical point, such as unusual power laws or a non-Fermi liquid behavior, can be observed at attainable temperatures.

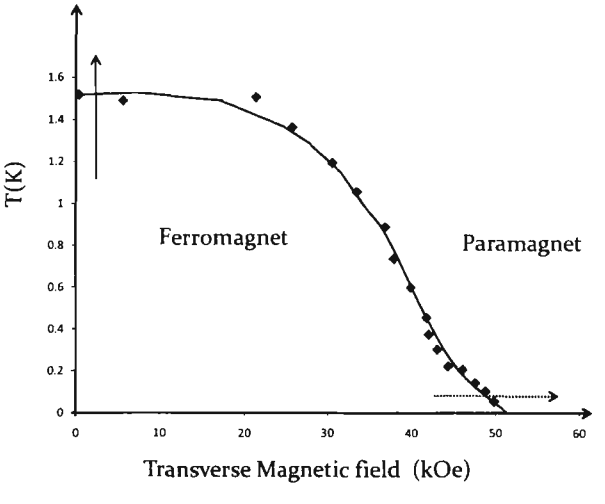

Figure 1.2. Magnetic phase diagram of $LiHoF_4$ as a function of temperature and external magnetic field. The solid and dotted arrows show phase transitions caused by thermal and quantum fluctuations respectively.

The schematic phase diagram in figure 1.3 shows the non-zero temperature effects of a quantum critical point. The external tuning parameter for this quantum phase transition is pressure. Quantum fluctuations dominate the quantum-paramagnetic region, whereas thermal fluctuations dominate the thermal-paramagnetic region. Both fluctuations become important in the quantum critical region. The crossover lines between the quantum critical region and both paramagnetic regions are determined by comparing the thermal energy $k_B T$ and the quantum energy $\hbar\omega_c$. The magnitude of the quantum energy can be estimated from the typical time scale (i.e., equation (2)) of quantum fluctuations. The dimensionless quantity describing the distance from the critical point at absolute zero is $r = (p - p_c)/p_c$, where p_c is the critical pressure. Since ω_c is proportional to $1/\tau_c$, the quantum energy is calculated as

$$\hbar\omega_c \propto |r|^{\nu z} \ . \tag{13}$$

Quantum fluctuations are important as long as the quantum energy is greater than the thermal energy. The boundaries of the quantum critical region are given by the condition $k_B T \sim |r|^{\nu z}$.

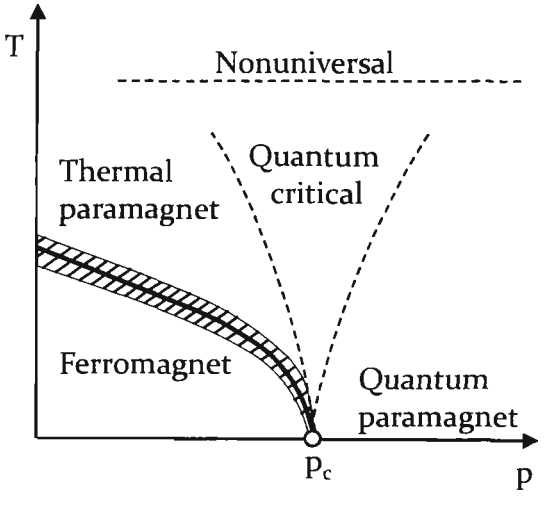

Figure 1.3. Phase diagram in the vicinity of a quantum critical point located at p_c, where p is the pressure and T is the temperature. The shaded region is the classical critical region.

Exciting the quantum critical ground state by increasing the temperature leads to unusual behavior in the quantum critical region.

Since thermal fluctuations dominate the shaded phase-boundary region in figure 1.3, this region is described by the classical theory. In such cases, the phase transition takes place at a finite temperature. Moreover, the quantum energy is less than the thermal energy, and although quantum fluctuations are present at a microscopic level, they do not control the critical behavior.

Figure 1.3 corresponds to a transition at which the ordered phase exists at non-zero temperatures. In some cases, it exists only at absolute zero. The schematic phase diagram in a such situation is similar to that in figure 1.3; however, the finite-temperature ferromagnetic region collapses on the pressure axis (see [17]).

The statistical mechanics approaches to classical and quantum phase transitions are similar. In the case of a classical Hamiltonian, where the kinetic part H_K depends on generalized momenta p_i and the potential part H_P depends only on the generalized coordinates q_i, the partition function can be written as

$$Z = \int \prod_i \mathrm{d}p_i e^{-H_K/k_BT} \int \prod_i \mathrm{d}q_i e^{-H_P/k_BT} \ . \tag{14}$$

The kinetic part of the partition function does not usually contribute to the singularity of the free energy density (i.e., equation (3)) since it has Gaussian terms and the Gaussian integrals are not singular. Therefore, phase transitions in such systems can be studied using a time-independent theory such as the Landau-Ginzburg-Wilson theory[12].

The statistical mechanics of a quantum phase transition in d dimension are closely related to those of a classical phase transition in $d+z$ dimension[13]. The mapping of a quantum phase transition onto a classical transition introduces an additional dimension of imaginary time. The reason is that the dynamics and the statics do not separate from each other for a quantum Hamiltonian in which the kinetic part H_K and the potential part H_P do not commute. In such a situation, the partition

[12]Discussed below in section 2.2.

[13]This concept is different from application of the classical theory to the shaded phase-boundary region in figure 1.3.

function can be rewritten by using Trotter decomposition[14], which introduces an extra dimension of the imaginary time $\tau = \beta = -i\Theta/\hbar$, where Θ is the real time. At a non-zero temperature transition, the imaginary time has a finite spread, and due to dominant thermal fluctuations, does not influence the asymptotic critical behavior. The imaginary time, however, has an infinite spread at a zero-temperature transition. Therefore, the quantum phase transition in d dimension can be mapped onto a classical transition in $d + z$ dimension[15], and the scaling hypothesis of equation (6) can be generalized to

$$f(r, h, T) = |r|^{(1/y+z)} \psi_{\pm} \left(h\,|r|^{-(x/y)}, T\,|r|^{-z} \right) . \tag{15}$$

The approach of mapping a quantum phase transition onto a classical phase is limited to the thermodynamics of a quantum phase transition since it rewrites the partition function. Other approaches are required to address other features such as finite-temperature real-time dynamics.

1.4. DISORDER AND DISSIPATION IN PHASE TRANSITIONS

A real solid always contains disorder in the form of lattice defects, imperfections, or impurities. The following discussion is limited to the simplest kind of disorder, which is time independent, it is also known as a quenched or frozen disorder. Moreover, the disorder is assumed to have no qualitative influence on any of the bulk phases. Such disorder is called weak or random-T_c disorder. An experimental example of weak disorder arises from doping of nonmagnetic atoms in a classical ferromagnet.

Under certain circumstances, weak disorder can influence a phase transition. Harris [21] found a condition under which the effects of weak disorder do not change critical behavior at a classical critical point. The same condition was later found to be applicable to quantum critical points. The Harris criterion states that a clean

[14]The Trotter decomposition [19, 20] simplifies the partition function in imaginary time as follows. The Trotter formula for operators $\hat{A}$ and $\hat{B}$ is $e^{\hat{A}+\hat{B}} = \lim_{N\to\infty} \left(e^{\frac{\hat{A}}{N}} e^{\frac{\hat{B}}{N}} \right)^N$. Thus, the kinetic and potential parts of the Hamiltonian are separated in the quantum case with an additional dimension of imaginary time.

[15]The dimension is $d + z$ and not $d + 1$ because time scales with the length as time$\sim$length^z.

critical point is stable against weak disorder if

$$d\nu > 2\,, \tag{16}$$

where d is the system dimension and ν is the correlation-length critical exponent. This condition is derived by considering partial regions of size ξ. Due to disorder, each region has a somewhat different critical temperature than the bulk critical temperature of the impure system. If the variation in the reduced temperature from region to region is smaller than the reduced temperature of the clean system (i.e., the system without disorder), then order-parameter fluctuations caused by the weak disorder are suppressed at the phase transition. The central limit theorem gives the local variation in the reduced system temperature, which is proportional to $\xi^{-d/2}$. Using the relationship between r and ξ, the local variation in the reduced system temperature can be rewritten as $r^{d\nu/2}$. Thus, the condition for the suppressed weak disorder is $r^{d\nu/2} < r$. This condition implies equation (16) at the critical point (i.e., $r \to 0$).

In a phase transition, violation of the Harris criterion creates three possibilities:

1. The critical behavior is affected such that the numerical value of the critical exponent ν changes to meet the criteria. Thus, conventional power law scaling is observed at the critical point, but with a different value of ν.

2. The disorder destroys the conventional critical behavior. It leads to non-power-law scaling behavior of the critical exponents. The disorder effects increase without limit at the critical point, which is called an infinite-randomness critical point. This scenario is discussed in chapter 3.

3. The disorder can destroy the phase transition completely. The system has independent regions that undergo phase change at different critical temperatures. Therefore, the transition is smeared (see [22]) over a temperature range.

Another consequence of disorder is Griffiths phases. An infinite disordered system can have large spatial regions with no impurities, and the probability of finding these regions is exponentially small. These regions, called rare regions, tend to undergo phase transition at the critical temperature of the clean system. The disordered

Griffiths phase[16] [23, 24] is the region in the parameter space between the critical temperature of a clean system and that of an impure system. An ordered Griffiths phase[17] also exists in the ordered phase of the transition. The dynamics of rare regions are slow because they require a change in the order parameter over a large volume. In the case of a classical system, rare regions contribute to the observed thermodynamic quantities in the form of a power law within their volume. Because the probability of finding these regions is exponentially small, the effects of Griffiths phases are weak in the quantities observed for a classical system; nevertheless, they are important for the long-term dynamics of a classical system. They are also important in a quantum system, where the contribution of rare regions to the observed quantities can be exponentially large within their volume.

Apart from disorder, dissipation influences the dynamics of a phase transition. Thus, order-parameter modes interact with other low-energy modes, creating a kind of 'friction force' similar to the damping force in a harmonic oscillator. Since dynamics and statics decouple in a classical phase transition, dissipation does not influence the transition. However, dissipation becomes important in a quantum phase transition in which dynamics and statics are coupled. Chapter 4 discusses experimental examples in which the effects of the disorder and the linear damping are apparent.

The reminder of the thesis is organized as follows: Chapter 2 discusses the Landau theory and presents the Landau-Ginzburg-Wilson theory for the classical Ising spin model. Chapter 3 addresses the renormalization group method and studies the strong-disorder renormalization group method by applying it to the transverse-field Ising model. The main part of the thesis begins with chapter 4, which first describes experiments involving quantum phase transitions with dissipation and disorder. This chapter continues discussing the Landau-Ginzburg-Wilson theory suitable for investigation of these quantum phase transitions. The strong-disorder renormalization group method is applied to this theory, and recursion relations and flow equations are derived to find observable quantities. Finally, chapter 5 considers an extension of the problem in which the Ohmic (i.e., linear) damping in the experimental examples is replaced by the super-Ohmic damping.

[16]The Griffiths phase is also known as the Griffiths region.

[17]For a review of this topic see, e.g., [22, 15]

2. THE ORDER PARAMETER FIELD THEORY

Initial attempts to describe phase transitions were of the mean-field theory[18] kind; that is, the interaction of a particle with the rest of the system was treated as the interaction with the average local field. The following discusses the Landau theory, which can be considered a unification of earlier mean-field theories.

2.1. LANDAU THEORY

Landau theory is based on the assumption that for a given phase transition, the free energy can be written as a power series expansion of the order-parameter's thermal average $\langle\phi\rangle$ [25, 26, 27, 28, 29]. In a continuous phase transition, the order parameter increases continuously from zero in the ordered phase. In a first-order phase transition, on the other hand, the order parameter changes discontinuously at the transition temperature. Because the series expansion is relevant under the assumption of a small order parameter near the phase transition, the Landau theory is better controlled for a continuous phase transition than for a first-order phase transition. The expansion of the Landau free energy F_L is

$$F_L = a_0 + a_2 \langle\phi\rangle^2 + a_3 \langle\phi\rangle^3 + a_4 \langle\phi\rangle^4 + O\left(\langle\phi\rangle^5\right) . \tag{17}$$

The values of parameters a_0, a_2, a_3, and a_4 [19] are determined by the system's degrees of freedom, which exclude the order parameter, and these are dependent on external parameters such as temperature and pressure. The physical value of the thermal average of the order parameter is obtained by minimizing the free energy.

---

[18] See e.g.,[13]

[19] The reason for the absence of a first-order term in the free energy expansion is that, depending on the value of a_2, the free energy minimum is located either in the ordered phase or in the disordered phase. The system's state is specified by a partial derivative of this absolute minimum, i.e.

$$\frac{\partial F_L}{\partial \langle\phi\rangle} = a_1 + 2a_2 \langle\phi\rangle + 3a_3 \langle\phi\rangle^2 + ... = 0 .$$

Since the order parameter vanishes in the disordered phase (i.e., $\langle\phi\rangle = 0$), the above equation is satisfied for the condition $a_1 = 0$; therefore, there is no first-order term in the Landau free energy expansion.

The Landau theory describes a first-order phase transition for $a_3 \neq 0$. For $a_2 > a_2^*$ (Figure 2.1(a)), where a_2^* is the value of a_2 at the phase transition, the absolute minimum of the free energy is located at $\langle\phi\rangle = 0$, and the system is in the disordered phase. The ordered phase appears as a second local minimum of the free energy, and at $a_2 = a_2^*$, where the Landau free energies of both phases coincide, it is located at $\langle\phi\rangle \neq 0$ (Figure 2.1(b)). For $a_2 < a_2^*$ (Figure 2.1(c)), the system is in the ordered phase, and the absolute minimum is located at $\langle\phi\rangle \neq 0$. In this case, the system jumps discontinuously from the disordered phase (i.e., $\langle\phi\rangle = 0$) to the ordered phase (i.e., $\langle\phi\rangle \neq 0$).

The Landau theory describes a continuous phase transition for $a_3 = 0$, which is usually due to symmetry. The critical point is located at $a_2 = 0$ (Figure 2.2(b)). In case of a thermal continuous-phase transition, a_2 gives the distance from the critical point (i.e., a_2 is proportional to $T - T_c$). For $a_2 > 0$, the system is in the disordered phase (Figure 2.2(a)).

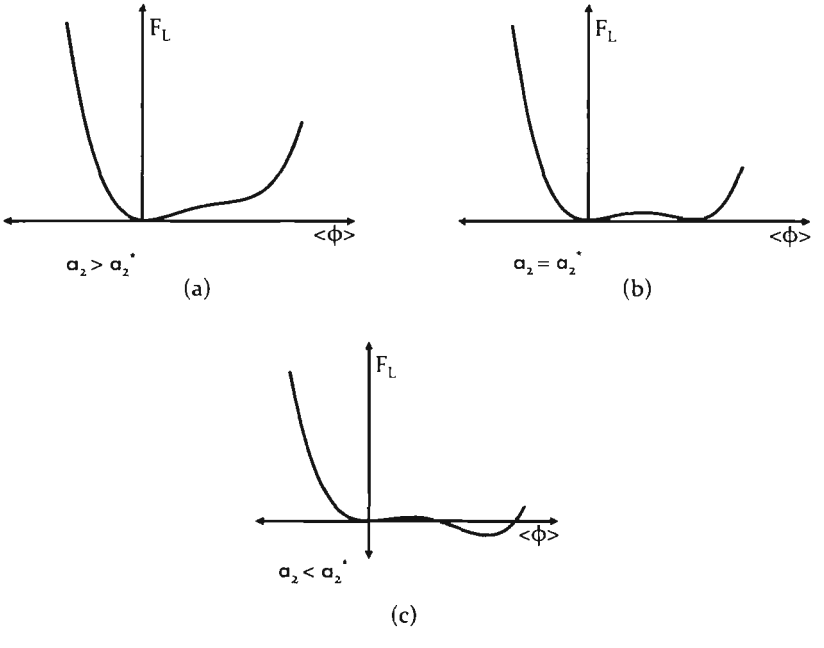

Figure 2.1. Landau free energy in a first-order transition: Landau free energy as a function of the order parameter's thermal average at (a) $a_2 > a_2^*$, (b) $a_2 = a_2^*$, and (c) $a_2 < a_2^*$.

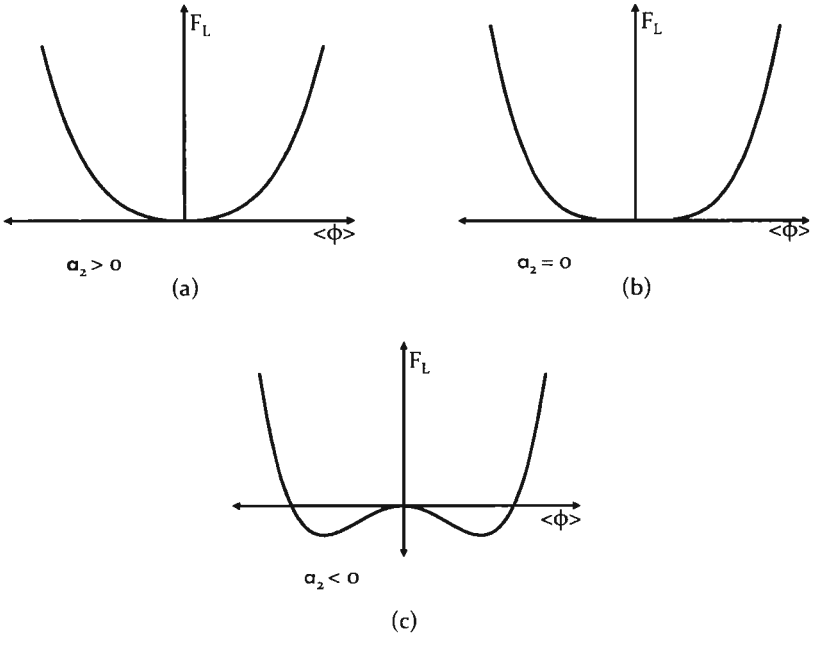

Figure 2.2. Landau free energy in a continuous phase transition: Landau free energy as a function of the order parameter's thermal average at (a) $a_2 > 0$, (b) $a_2 = 0$, and (c) $a_2 < 0$.

In equation (17), if the term $\langle\phi\rangle^5$ and higher order terms are disregarded, then the minimum of free energy is located in the ordered phase at $\langle\phi\rangle = \pm\sqrt{\frac{-a_2}{2a_4}}$, as shown in Figure 2.2(c). Thus, the critical exponent β predicted by the Landau theory is 1/2. For a non-zero field h, which is conjugate to the order parameter, equation (17) has an extra term of $-h\langle\phi\rangle$. The partial derivative of this free energy with respect to the order parameter's thermal average then gives

$$2a_2\langle\phi\rangle + 4a_4\langle\phi\rangle^3 = h\ . \tag{18}$$

Using this equation of state, the Landau theory gives the critical exponents γ, α, and δ. For example, the magnetic susceptibility can be found by differentiating equation (18) with respect to h (i.e., $\chi = \partial\langle\phi\rangle/\partial h$). This differentiation, in turn, gives

$$\chi \propto |a_2|^{-1} \propto |T - T_c|^{-1}\ . \tag{19}$$

Thus, the critical exponent γ predicted by the Landau theory is 1. Similarly, α is equal to 0 and δ is equal to 3.

The Landau theory uses the order-parameter mean while neglecting order-parameter fluctuations about the mean. It can fail near the critical point regime, where order-parameter fluctuations about the mean are significant. The dominance of fluctuations usually decreases as the system dimension and the number of order-parameter components increases. Ginzburg found that the Landau theory breaks down below a certain dimension d_c^+, which is the upper critical dimension [30, 31]. This dimension is independent of the number of order-parameter components. Therefore, magnetic systems of Ising and Heisenberg spin symmetries have the same upper critical dimension (i.e., $d_c^+ = 4$). The lower critical dimension d_c^- gives the limit below which no phase transition is observed in the system. In such a case, no long range order is possible due to strong fluctuations. The lower critical dimension is 1 for the Ising and 2 for the Heisenberg spin symmetry.

At the phase boundary, fluctuations become important in a system of dimension d, where $d_c^- < d < d_c^+$; accordingly, modifications in the Landau theory become necessary, as discussed in section 2.2.

2.2. LANDAU-GINZBURG-WILSON THEORY

A theory that includes fluctuations, at least those at the long wavelengths, is required to describe phase transitions for $d < d_c^+$, the region where the Landau theory fails. The Landau-Ginzburg-Wilson theory proposes a free-energy functional[20] that considers long-wavelength order-parameter fluctuations. The free-energy functional can be derived from a microscopic Hamiltonian or developed from symmetry considerations. The following discusses the difference in formalism between a classical and a quantum Hamiltonian.

[20] A functional is a function of a function. It is also referred to as an action in the quantum field theory.

The Landau-Ginzburg-Wilson theory of a classical (thermal) transition [21] can be written as

$$Z = \int \mathrm{D}(\phi)\, e^{-S[\phi(\mathbf{x})]} = \prod_{\mathbf{x}} \int \mathrm{d}\phi(\mathbf{x})\, e^{-S[\phi(\mathbf{x})]}\,, \tag{20}$$

where $S[\phi(\mathbf{x})]$ is the Landau-Ginzburg-Wilson functional. For the simplest case of a scalar order parameter, $S[\phi(\mathbf{x})]$ in d dimension is

$$S[\phi(\mathbf{x})] = \frac{1}{k_B T} \int \mathrm{d}^d\mathbf{x}\, [\xi_0^2\, (\nabla\phi(\mathbf{x}))^2 + F_L(\phi(\mathbf{x}))]\,, \tag{21}$$

where $F_L(\phi(\mathbf{x}))$ is the Landau free energy, and ξ_0 is a microscopic length scale. The order parameter average $\phi(\mathbf{x})$ is defined at the center position $\mathbf{x}$ of a cell. The size of the cell is usually larger than the distance between the particles or the range of their interaction. In the above functional, rapid order-parameter fluctuations are restricted by the term $(\nabla\phi(\mathbf{x}))^2$. This term is relevant near the critical point, where the order parameter has long-wavelength fluctuations.

The Landau-Ginzburg-Wilson functional is formulated in space and imaginary time variables for a quantum Hamiltonian, the kinetic and the potential parts of which cannot be separated. The partition function is

$$Z = \prod_{\mathbf{x},\tau} \int \mathrm{d}\phi(\mathbf{x},\tau)\, e^{-S[\phi(\mathbf{x},\tau)]}\,. \tag{22}$$

As an example, the Landau-Ginzburg-Wilson functional for a d dimensional quantum Hamiltonian could be

$$S[\phi(\mathbf{x},\tau)] = \int_0^{\frac{1}{k_B T}} \mathrm{d}\tau \int \mathrm{d}^d\mathbf{x} \left[\tau_0^2 \left(\frac{\partial\phi(\mathbf{x},\tau)}{\partial\tau}\right)^2 + \xi_0^2\, (\nabla\phi(\mathbf{x},\tau))^2 + F_L(\phi(\mathbf{x},\tau))\right], \tag{23}$$

where τ_0 is a microscopic time scale. The coefficients ξ_0 and τ_0 depend on the degrees of freedom other than the order parameter.

[21] The partition function of this transition can be described by a time-independent formalism of equation (14) in section 1.3.

The Landau-Ginzburg-Wilson functional for the Ising model is derived here as an example. The Hamiltonian for the classical one-dimensional Ising model of N sites with no external field is

$$H = -\frac{1}{2}\sum_{ij} J_{ij}\, S_i S_j \ , \tag{24}$$

where S_i, $S_j = \pm 1$ are the classical Ising spins at neighboring sites i and j with the interaction J_{ij}. The partition function, then, is

$$Z = \sum_{\pm 1} e^{-\beta H} = \sum_{\pm 1} e^{\frac{1}{2}\sum_{ij} P_{ij} S_i S_j} \ , \tag{25}$$

where P_{ij} is equal to βJ_{ij}. By applying the Hubbard-Stratanovich transformation [32, 33], the partition function can be written in terms of a classical field ϕ as

$$Z = C \int_{-\infty}^{\infty} \left(\prod_{i=1}^{N} \mathrm{d}\phi_i \right) e^{-\frac{1}{2}\sum_{ij} \phi_i P_{ij}^{-1} \phi_j} \sum_{\pm 1} e^{\sum_i \phi_i S_i} \ , \tag{26}$$

where C is equal to $(\det P_{ij}/(2\pi)^N)^{1/2}$. Since the spin part is formally noninteracting, S_i can be integrated out, leading to the Landau-Ginzburg-Wilson functional expressed as

$$S(\phi) = \frac{1}{2}\sum_{ij} \phi_i P_{ij}^{-1} \phi_j - \sum_i \ln(2\cosh(\phi_i)) \ . \tag{27}$$

The fourier transform of $\mathbf{P}$, where $\mathbf{P}$ is an $N \times N$ matrix (the only non-zero elements of which represent nearest neighbor interaction), is

$$\tilde{\mathbf{P}}(\mathbf{q}) = 2P\cos(\mathbf{q}a) \ ,$$

where a is the lattice spacing and P is equal to βJ. Therefore, for the long wavelengths of the order parameter, $\tilde{\mathbf{P}}^{-1}(\mathbf{q})$ is approximately equal to $a^2\mathbf{q}^2/4P$, where the constants are absorbed in the Landau free energy expansion. The second term of equation (27) can be simplified by expanding the logarithmic term for small values of $\phi^2/2$ in the hyperbolic cosine expansion. Thus, the Landau-Ginzburg-Wilson

functional in the fourier space is

$$S[\phi(\mathbf{q})] = \int \mathrm{d}\mathbf{q}\,[\xi_0'^2\,(\phi(\mathbf{q})\mathbf{q}^2\phi(\text{-}\mathbf{q})) + F_L(\phi(\mathbf{q}))]\,,$$

which is equation (21) for $d = 1$ in the fourier space.

Finding the critical exponents in the Landau theory is simple; however, the Landau-Ginzburg-Wilson theory has complications of interacting many-particle system. The renormalization group is used to solve the functional and thus to obtain the critical exponents. Chapter 3 discusses the renormalization group method.

3. STRONG-DISORDER RENORMALIZATION GROUP METHOD

One of the methods used to study a zero-temperature phase transition in the presence of disorder is the strong-disorder renormalization group method [34]. Initially, this method was introduced to study random Heisenberg antiferromagnetic spin chains [35, 36]. The following provides an introduction to renormalization group methods in general (see, e.g., [37, 4, 38, 39]).

3.1. RENORMALIZATION GROUP METHOD

The renormalization group method is based on the notion that at the critical point, a system looks identical at all length scales. Correlation-length divergence at the critical point indicates dominance of long-wavelength order-parameter fluctuations. Essentially, the renormalization group method eliminates the degrees of freedom that do not contribute to the critical behavior. In other words, the degrees of freedom contributing to short-wavelength order-parameter fluctuations are eliminated by the coarse graining technique. After eliminating these degrees of freedom, a new Hamiltonian is written, which retains the old form, but has a reduced number of degrees of freedom. This new Hamiltonian is subjected to the same procedure and so on, which reveals the system at various length scales. Recursion relations that describe the changes in the Hamiltonian's parameters (i.e., coupling constants) under coarse graining are derived in this process. Infinite iterations of the recursion relations are carried out so that the unusual behavior of the system can be observed in the thermodynamic limit. The system behavior is studied in the parameter space, where the coupling constants are its axes. In this space, the iterative mapping results in the flow of the Hamiltonian. At the end of the process, the system may be found at a fixed point, where the point is mapped onto itself. A fixed point can be attractive, repulsive, or mixed. If the system starts near an attractive fixed point, then the iterations bring it back to the fixed point. On the other hand, if the system starts near a repulsive fixed point, it is driven away from that by the iterations. If the fixed point is mixed, the system is attracted in one direction and repelled in another direction. The various phases of the system are represented by stable fixed points. A

fixed point that is repulsive in one direction and attractive in all other directions is a critical point. Since the critical point is unstable in only one direction, the system can be brought to this point by tuning only one parameter. The correlation length can go to either zero or infinity at a fixed point. The latter case represents the critical point.

3.2. STRONG-DISORDER RENORMALIZATION GROUP METHOD

Renormalization group methods can be performed either in the Fourier space or in the real space. The strong-disorder renormalization group method belongs to the latter case. Although this method is considered a real-space renormalization group method, it is based on energy considerations. In a real-space renormalization method, the coarse graining procedure (e.g., in a magnetic system), consists in replacing a block of a few lattice spins by a single spin. All sites in a system having the disorder cannot be treated on the same footing. To overcome this problem, the coarse graining technique is developed such that the degrees of freedom contributing to high-energy modes are eliminated while the degrees of freedom that contribute to low-energy modes of the system are retained.

As discussed in section 1.4 above, three types of disorder behavior are possible in a system under the coarse graining method:

1. The disorder can approach a finite limit, leading the system to a finite-randomness (or disorder) fixed point.

2. The disorder can increase without limit, leading the system to the fixed point known as an infinite-randomness fixed point.

3. The disorder can decrease and eventually vanish, leading the system to a clean fixed point.

The strong-disorder renormalization group method works particularly well in the second case because it relies on the breadth of the disorder distributions. In the following discussion, this method is applied to a quantum mechanical toy model for the magnetic behavior of $LiHoF_4$ [40] to illustrate its operation.

The Hamiltonian of the transverse-field Ising-spin chain model is given by

$$H = -\sum_i J_i \hat{\sigma}_i^z \hat{\sigma}_{i+1}^z - \sum_i h_i \hat{\sigma}_i^x \ , \tag{28}$$

where $J_i > 0$ is the coupling (i.e., nearest neighbor interaction) and $h_i > 0$ is the transverse field at a lattice site i. The quantum spin operators $\hat{\sigma}^z$ and $\hat{\sigma}^x$ are represented by the Pauli matrices:

$$\hat{\sigma}^x = \begin{pmatrix} 0 & 1 \\ 1 & 0 \end{pmatrix} \ , \ \hat{\sigma}^y = \begin{pmatrix} 0 & -i \\ i & 0 \end{pmatrix} \ , \ \hat{\sigma}^z = \begin{pmatrix} 1 & 0 \\ 0 & -1 \end{pmatrix} \ . \tag{29}$$

For the operator $\hat{\sigma}^z$, Ising spin has two orthogonal eigenstates, $|\uparrow\rangle$ and $|\downarrow\rangle$. In the matrix representation, these are

$$|\uparrow\rangle = \begin{pmatrix} 1 \\ 0 \end{pmatrix} \ , \ |\downarrow\rangle = \begin{pmatrix} 0 \\ 1 \end{pmatrix} \ . \tag{30}$$

Likewise, for the operator $\hat{\sigma}^x$, Ising spin has two orthogonal eigenstates, $|\rightarrow\rangle$ and $|\leftarrow\rangle$, which can be written as

$$|\rightarrow\rangle = \frac{|\uparrow\rangle + |\downarrow\rangle}{\sqrt{2}} \ , \ |\leftarrow\rangle = \frac{|\uparrow\rangle - |\downarrow\rangle}{\sqrt{2}} \ . \tag{31}$$

The first term in equation (28) represents the interaction between the z components of neighboring spins. When there is no transverse field (i.e., when h_i is equal to 0), all spins tend be in either the $|\uparrow\rangle$ or $|\downarrow\rangle$ eigenstate. The result is a ferromagnetic phase. When the transverse field is turned on (i.e., when h_i is not equal to 0), tunneling is induced between those two eigenstates, an effect that destroys the parallel spins. Because all spins are pointing in **x** direction at a sufficiently large field, the system turns into the paramagnetic phase. The competition between couplings J_is and fields h_is at the lattice sites thus leads to paramagnetic-ferromagnetic quantum phase transition.

The following discussion considers a disordered version of this model, that is, a model in which h_i and J_i are drawn from some random distribution. The procedure for applying the strong-disorder renormalization group method to this model is as

follows [40, 41]: The first step is to identify the largest local energy in the system (i.e., $\Omega = \max(J_i, h_i)$). Among all J_i and h_i of the Hamiltonian, the largest is considered first. The largest energy can be either a coupling between any two neighboring sites or a field at a site. If a coupling e.g., J_3 is the largest energy, the next step is to find the ground state of the associated cluster. The unperturbed Hamiltonian $-J_3\hat{\sigma}_3^z\hat{\sigma}_4^z$ has a twofold degenerate ground state. The degenerate ground eigenstates are $|\uparrow\uparrow\rangle$ and $|\downarrow\downarrow\rangle$. The field terms at sites 3 and 4 (i.e., $-h_3\hat{\sigma}_3^x - h_4\hat{\sigma}_4^x$) are treated by the second-order degenerate perturbation theory. The excited states involving the coupling are then eliminated, and the new Hamiltonian is written with a reduced number of degrees of freedom. Thus, the excited states of the cluster $|\uparrow\downarrow\rangle$ and $|\downarrow\uparrow\rangle$ involving J_3 are eliminated. Consequently, the spins at sites 3 and 4 are collectively treated as a single spin with a magnetic moment equal to the sum of the magnetic moments of the combined spins. Using this effective spin, the new Hamiltonian is written as $-\tilde{h}_3\hat{\sigma}_3^x$ with the field $\tilde{h}_3$ given by

$$\tilde{h}_3 \approx \frac{h_3 h_4}{J_3} \,. \tag{32}$$

For the effective spin, the spin operator in the transverse direction x is assumed to be the same as that of the spin at site 3. Likewise, the spin operator along the z direction is assumed to be similar to that of the spin at site 3. The Hamiltonian for the couplings of the effective spin is then written as $-J_2\hat{\sigma}_2^z\hat{\sigma}_3^z - J_4\hat{\sigma}_3^z\hat{\sigma}_5^z$. These assumptions are valid if J_3 is much greater than h_3 and h_4. Hence, a Hamiltonian is obtained with a reduced number of degrees of freedom and a lower value of the maximum energy Ω.

If a field e.g., h_3 is the largest energy in the system, then the unperturbed Hamiltonian is $-h_3\hat{\sigma}_3^x$. The couplings between sites 3 and 2, and those between sites 3 and 4 (i.e., $-J_2\hat{\sigma}_2^z\hat{\sigma}_3^z - J_3\hat{\sigma}_3^z\hat{\sigma}_4^z$) are treated by the second-order degenerate perturbation theory. The spin at site 3 is then eliminated, along with its excited state $|\leftarrow\rangle$ involving the field. Consequently, the spins at sites 2 and 4 are joined by the effective coupling $\tilde{J}_2$, where

$$\tilde{J}_2 \approx \frac{J_2 J_3}{h_3} \,. \tag{33}$$

Thus, as in the earlier case, the process yields a new Hamiltonian with a reduced number of degrees of freedom and a lower value of Ω. These steps are repeated ad infinitum.

If a coupling is the largest energy, its elimination favors cluster formation. Therefore, the iterative procedure of eliminating couplings leads to growth of the cluster size while the maximum energy of the system goes to zero. These conditions lead the system to the ferromagnetic phase. A cluster of infinite size is formed at $\Omega = 0$. In contrast, if a field is the largest energy, its elimination hinders cluster formation. Thus, the iterative procedure of eliminating fields does not form a cluster, and with Ω tending to 0, the system goes into the paramagnetic phase.

The probability distribution functions of $\ln J$ and $\ln h$ change with the recursion relations (32) and (33). The flow equations for these distributions under repeated elimination of couplings and fields can be derived as explained in [41]. The solution of the flow equations gives three kinds of nontrivial fixed points, among which is a line of fixed points representing the quantum Griffiths paramagnet and another one representing the quantum Griffiths ferromagnet. The fixed point, which separates these two lines, is the quantum critical point.

At the critical point, the length scale L of a surviving cluster is given by

$$L^{\psi} \approx \ln\left(\frac{\Omega_0}{\Omega}\right) , \tag{34}$$

where Ω_0 is the initial energy of the system and ψ is the so-called tunneling critical exponent defined by

$$\tau_c \propto \exp \xi^{\psi} . \tag{35}$$

In this model, ψ is equal to 1/2. The correlation-length scaling law is given by $\xi \approx |r|^{-\nu}$. The distance from the critical point r is defined as

$$r = \frac{\overline{\ln h} - \overline{\ln J}}{\mathrm{var}\,(\ln h) + \mathrm{var}\,(\ln J)} , \tag{36}$$

where $\overline{\ln h}$ and $\overline{\ln J}$ are the averages and $\mathrm{var}\,(\ln h)$ and $\mathrm{var}\,(\ln J)$ are the variances of the probability distribution functions. In this model, ν is equal to 2. Near the

infinite randomness critical point, the width of probability distributions of the coupling constants tend to infinity, justifying the method. If the spins are located at a specific distance, the resulting spin-spin correlation functions differ for those belonging to different clusters and for those belonging to a single cluster. This result causes variations in the typical and average values of physical quantities. Chapter 4 elaborates on these results, deriving recursion relations similar to equations (32) and (33).

4. DISORDER AND DAMPING IN QUANTUM PHASE TRANSITION

The main topic of the thesis is discussed in this chapter. The initial discussion is about the motivation for this study of quantum phase transitions with disorder and ohmic damping.

4.1. THE EXPERIMENTAL MOTIVATION

Following are three examples of quantum phase transitions exhibiting complex phenomena, including non-Fermi liquid behavior[22] of observable quantities at low temperatures.

4.1.1. Quantum phase transition in $CePd_{1-x}Rh_x$. The tuning parameter of the quantum ferromagnetic-paramagnetic transition in $CePd_{1-x}Rh_x$ (i.e., cerium-palladium-rhodium) is chemical composition. Figure 4.1 shows a temperature-concentration phase diagram of this substance [44]. Pure CePd undergoes a thermal ferromagnetic-paramagnetic transition at 6.6°K.

[22] An extensive list of experiments in non-Fermi liquid behavior can be found in [42, 43].

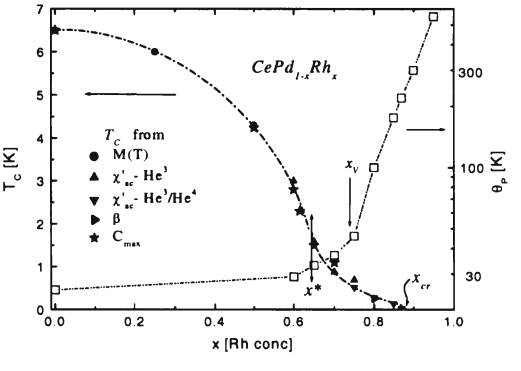

Figure 4.1. Magnetic phases of $CePd_{1-x}Rh_x$ as a function of temperature and rhodium concentration. Various techniques for measuring critical temperature measurements are listed. The phase boundary has an unusual shape beyond a rhodium concentration of 0.65. (Reprinted figure with permission from J. G. Sereni, T. Westerkamp, R. Küchler, N. Caraco-Canales, P. Gegenwart, and C. Geibel, Physical Review B, 75, 024432 (2007). Copyright (2007) by the American Physical Society.)

Rhodium forms a nonmagnetic ground state with the cerium; therefore, the ferromagnetic phase of the substance gets suppressed as the concentration of rhodium increases and that of palladium decreases. The shape of the phase boundary is unusual beyond a 0.65 concentration of rhodium. The apparent quantum critical point, x_{cr}, is at a concentration of approximately 0.87. Figure 4.2 shows the susceptibility measurements as a function of temperature for various concentrations in the tail of the ferromagnetic phase [45]. The susceptibility can be fitted above the phase boundary by a nonuniversal power law, which is predicted by the quantum Griffiths scenario[23]. In this quantum phase transition, the disorder is due to random positions of the rhodium atoms; the magnetization modes are damped by the conduction electrons because the system is metallic in both phases.

4.1.2. Quantum phase transition in $Ni_{1-x}V_x$. Nickel undergoes a thermal ferromagnetic-paramagnetic transition at 630°K. The critical temperature drops as the concentration of vanadium increases and that of nickel decreases.

[23]See section 1.4.

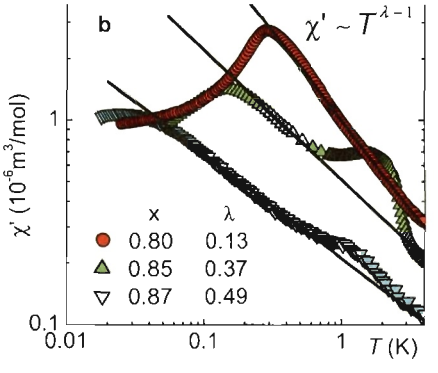

Figure 4.2. Magnetic susceptibility of $CePd_{1-x}Rh_x$: The log-log plot of the susceptibility as a function of temperature near the critical concentration of rhodium. The term α is the Griffiths exponent with d as the system dimension and z as the dynamical critical exponent. (Reprinted figure with permission from T. Westerkamp, M. Deppe, R. Küchler, M. Brando, C. Geibel, P. Gegenwart, A. P. Pikul, and F. Steglich, Physical Review Letters, 102, 206404 (2009). Copyright (2009) by the American Physical Society.)

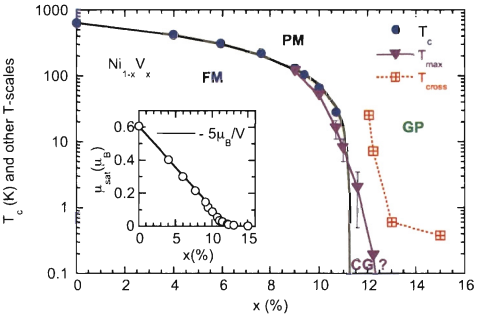

Figure 4.3. Magnetic phases of $Ni_{1-x}V_x$ as a function of temperature and Vanadium concentration showing ferromagnetic, paramagnetic and Griffiths paramagnetic regions. (Reprinted figure with permission from Sara Ubaid-Kassis, Thomas Vojta, and Almut Schroeder, Physical Review Letters, 104, 066402 (2010). Copyright (2010) by the American Physical Society.)

The system undergoes a quantum phase transition at a vanadium concentration of 11.4%, as shown in figure 4.3. Figure 4.4 [46] shows the susceptibility of $Ni_{1-x}V_x$ as a function of temperature for various Vanadium concentrations. For temperatures above 10 K, the susceptibility can be described by nonuniversal power law (i.e., χ is proportional to $T^{-\gamma}$). The disorder in this system arises from random positions of vanadium atoms, and the damping of magnetization modes is caused by conduction electrons.

4.1.3. Quantum phase transition in a superconducting nanowire. Extremely thin nanowires made for example of MoGe, undergo a quantum phase transition from a metallic to a superconducting state as a function of their thickness [47, 48]. The magnetic impurities on the surface of the wire are believed to destroy the superconducting phase. In this transition, the disorder arises from random positions of magnetic impurities on the wire surface, and the damping of pairing modes is again caused by conduction electrons.

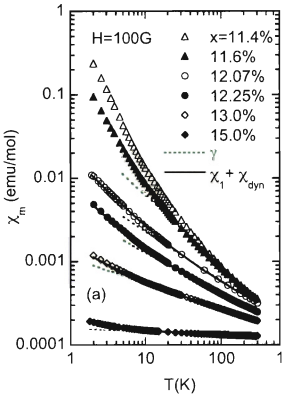

Figure 4.4. Magnetic susceptibility of $Ni_{1-x}V_x$ as a function of temperature near the critical concentration of Vanadium. (Reprinted figure with permission from Sara Ubaid-Kassis, Thomas Vojta, and Almut Schroeder, Physical Review Letters, 104, 066402 (2010). Copyright (2010) by the American Physical Society.) The dotted lines show power laws for $T > 10$°K. The solid lines represent a model that sums the Curie term and the quantum Griffiths law (see [46] for more details).

4.2. LANDAU-GINZBURG-WILSON THEORY

The following derives from a single-band electron model the Landau-Ginzburg-Wilson functional for a quantum phase transition in the presence of disorder and damping. The discussion focuses first on the origin of single-band model [24] and the motivation for using this model.

4.2.1. The Anderson and Kondo models. The transition metal (lanthanides and actinides) compounds studied here usually have more than one electron band close to the Fermi surface. In such compounds, these bands could be an s-band and a d-band. Anderson proposed a model to describe the interplay between two such bands in the presence of Coulomb interaction. This so-called *periodic Anderson model* or $s-d$ *model*[25] cannot be solved, therefore, a single impurity is considered to simplify the problem. The single-impurity Anderson model [52] considers magnetic moment formation caused by doping a single impurity in a nonmagnetic metal. The

[24] See, e.g., [49, 50]
[25] See, e.g., [51]

model treats valance electrons of the host metal as a band. An impurity is treated as a localized electron orbital that can be occupied by up to two electrons. The Hamiltonian of this model is

$$H = \sum_{\mathbf{k}s} \epsilon_{\mathbf{k}} C^{\dagger}_{\mathbf{k}s} C_{\mathbf{k}s} + \sum_{s} \epsilon_d \, n_{ds} + \sum_{\mathbf{k}s} V_{\mathbf{k}d} \left(C^{\dagger}_{\mathbf{k}s} c_{ds} + c^{\dagger}_{ds} C_{\mathbf{k}s} \right) + U \, n_{d\uparrow} n_{d\downarrow} \, , \qquad (37)$$

where $C^{\dagger}_{\mathbf{k}s}$ and $c^{\dagger}_{ds}$ are creation operators that create an electron of spin s in $\mathbf{k}$ state of conduction band and the impurity state d respectively. Likewise, $C_{\mathbf{k}s}$ and c_{ds} are annihilation operators that destroy an electron of spin s in the band and the impurity state. The term $\epsilon_{\mathbf{k}}$ is the band-electron energy in $\mathbf{k}$ state. An impurity electron has energy of ϵ_d. Its number operator, n_{ds}, is equal to $c^{\dagger}_{ds} c_{ds}$. The term $V_{\mathbf{k}d}$, which is a hybridization, represents a transition of an electron between the impurity state and a $\mathbf{k}$ state. The Coulomb interaction between the electrons in the impurity state is given by

$$U = \int \mathrm{d}\mathbf{x}_1 \, \mathrm{d}\mathbf{x}_2 \, |\phi_d(\mathbf{x}_1)|^2 \, \frac{e^2}{|\mathbf{x}_1 - \mathbf{x}_2|} \, |\phi_d(\mathbf{x}_2)|^2 \, , \qquad (38)$$

where the orbital wave function is represented by $\phi_d(\mathbf{x})$.

Hubbard estimated magnitudes of interactions between electrons in the impurity state [53]. The single-impurity Anderson model considers Coulomb repulsion between impurity electrons. This repulsion favors formation of local moments. The model discards both the Coulomb interaction between the impurity electrons at neighboring sites and the exchange interaction[26].

Formation of local moments and the resulting characteristics of a metal at low temperatures differ from those at high temperatures. This distinction is caused by the spin interaction between an impurity electron and a band electron. Hence, the model proposed by Kondo for this low temperature phenomenon discards charge fluctuations in the impurity state and considers only spin fluctuations. The Hamiltonian of this

[26]The electron exchange interaction results from electrons of similar spin orientations exchanging their spatial coordinates (see, e.g., [54]).

model is

$$H = \sum_{\mathbf{k}s} \epsilon_{\mathbf{k}} C^{\dagger}_{\mathbf{k}s} C_{\mathbf{k}s} - \sum_{\mathbf{k},\mathbf{k}'} J_{\mathbf{k},\mathbf{k}'} \left(C^{\dagger}_{\mathbf{k}} \hat{\sigma} C_{\mathbf{k}'} \right) \cdot \left(c^{\dagger}_{d} \hat{\sigma} c_{d} \right), \tag{39}$$

where $\hat{\sigma}$ is equal to $\frac{1}{2}\left[\hat{x}\hat{\sigma}^x + \hat{y}\hat{\sigma}^y + \hat{z}\hat{\sigma}^z\right]$ and $\hbar$ is equal to 1. The terms $\hat{\sigma}^x$, $\hat{\sigma}^y$, and $\hat{\sigma}^z$ are Pauli matrices. A singlet state formed by the interaction between a conduction band electron and an impurity electron at low temperatures is called the *Kondo effect.*

Here the Kondo effect is assumed to be present at low temperatures in a quantum phase transition.[27] This effect leads to the formation of heavy quasi-particles, which bear spins of impurity electrons, near the Fermi surface. These particles possess degrees of freedom relevant to the quantum phase transition. Hence, a single-band model of these particles is used to represent the problem.

4.2.2. Derivation of the Landau-Ginzburg-Wilson functional for ferromagnetic quantum phase transition. The standard techniques of [57, 58, 59] are used here to derive the Landau-Ginzburg-Wilson functional from a single-band microscopic model of interacting electrons. The steps of this derivation are outlined in section 2.2 above. Although, Hamiltonian formalism [57] can be used to derive this functional, the partition function representation in terms of Grassman fields [60] provides a more convenient approach. The partition function is

$$Z = \int \mathrm{D}\bar{\psi}_i(\mathbf{x},\tau)\, \mathrm{D}\psi_i(\mathbf{x},\tau)\, e^{-S} ,$$

where $\bar{\psi}_i(\mathbf{x},\tau)$ and $\psi_i(\mathbf{x},\tau)$ are Grassman fields (i.e., anticommuting numbers) defined at a position $\mathbf{x}$ and imaginary time τ with spin state i, which can be $\uparrow$ or $\downarrow$. The term $\mathrm{D}\bar{\psi}_i(\mathbf{x},\tau)\, \mathrm{D}\psi_i(\mathbf{x},\tau)$ is the Grassman functional integral measure. The functional S is the sum of functionals for free fermions S_0 and their interaction[28] S_I given by

$$S_0 = \int \mathrm{d}\mathbf{x} \int_0^{\beta} \mathrm{d}\tau \left[\bar{\psi}_i(\mathbf{x},\tau) \left(\frac{\nabla^2}{2m} + \mu \right) \psi_i(\mathbf{x},\tau) + \bar{\psi}_i(\mathbf{x},\tau) \frac{\partial}{\partial \tau} \psi_i(\mathbf{x},\tau) \right] \tag{40}$$

[27] There are systems in which the Kondo effect is not observed at low temperatures. On this topic, see reviews [55, 56].

[28] Since the derivation here is for a ferromagnetic-paramagnetic transition, it considers only the spin-triplet interaction, which results in the ferromagnetic phase. This formulation omits spin-singlet and Cooper pair interactions [61]. The field theory derivation for a ferromagnet differs for a Fermi liquid from that for a Fermi gas [62, 63]; for simplicity, here the derivation is only for a Fermi gas.

and

$$S_I = u \int \mathrm{d}\mathbf{x} \int_0^\beta \mathrm{d}\tau \, n_\uparrow(\mathbf{x},\tau) n_\downarrow(\mathbf{x},\tau) \,, \tag{41}$$

where m, which is set equal to 1, is the mass of an electron, μ is the chemical potential, β is equal to $1/k_B T$, and u is a constant. The number density n_i is equal to $\bar{\psi}_i \psi_i$. Use of equation (A.1) in the continuum space expresses equation (41) as

$$S_I = u' \int \mathrm{d}\mathbf{x} \int_0^\beta \mathrm{d}\tau \, \mathbf{n}_s(\mathbf{x},\tau) \cdot \mathbf{n}_s(\mathbf{x},\tau) \,, \tag{42}$$

where $\mathbf{n}_s(\mathbf{x},\tau)$ is a spin-density vector and u' is a constant.

The thermal average of contribution of spin-triplet interaction to the functional is given by

$$\langle e^{-S_I} \rangle_{S_0} = \frac{\int \mathrm{D}\bar{\psi}_i(\mathbf{x},\tau) \, \mathrm{D}\psi_i(\mathbf{x},\tau) \, e^{-S_0} \, e^{-S_I}}{\int \mathrm{D}\bar{\psi}_i(\mathbf{x},\tau) \, \mathrm{D}\psi_i(\mathbf{x},\tau) \, e^{-S_0}} \,.$$

If Z_0 is equal to $\int \mathrm{D}\psi_i^\dagger(\mathbf{x},\tau) \, \mathrm{D}\psi_i(\mathbf{x},\tau) \, e^{-S_0}$, then the partition function is

$$Z = Z_0 \, \langle e^{-S_I} \rangle_{S_0} \,.$$

Because Z_0 does not contribute to critical behavior, the singular part of the partition function is

$$Z \approx \langle e^{-S_I} \rangle_{S_0} \,. \tag{43}$$

The spin-triplet interaction is decomposed using the Hubbard-Stratanovich transformation, as shown in section 2.2 above. This decomposition yields the thermal average in terms of an order-parameter field, $\varphi(\mathbf{x},\tau)$:

$$\langle e^{-S_I} \rangle_{S_0} = \int \mathrm{d}\varphi(\mathbf{x},\tau) \, \mathrm{d}\varphi^*(\mathbf{x},\tau) e^{-\int \mathrm{d}\mathbf{x} \int_0^\beta \mathrm{d}\tau \, |\varphi(\mathbf{x},\tau)|^2} \langle e^{-\sqrt{u'} \int \mathrm{d}\mathbf{x} \int_0^\beta \mathrm{d}\tau \, \mathbf{n}_s(\mathbf{x},\tau) \cdot \varphi(\mathbf{x},\tau)} \rangle_{S_0} \,.$$

Use of expansion in terms of cumulants (i.e., equation (B.1)) simplifies the thermal

average. Because for noninteracting fermions

$$\left\langle -\int \mathrm{d}\mathbf{x} \int_0^\beta \mathrm{d}\tau \, \sqrt{u'}\, \mathbf{n}_s(\mathbf{x},\tau) \cdot \varphi(\mathbf{x},\tau) \right\rangle_{S_0} = 0 \, ,$$

the partition function is equal to

$$\int \mathrm{d}\varphi(\mathbf{x},\tau)\, \mathrm{d}\varphi^*(\mathbf{x},\tau) e^{-\int \mathrm{d}\mathbf{x} \int_0^\beta \mathrm{d}\tau\, |\varphi(\mathbf{x},\tau)|^2 + 2u' \langle \int \mathrm{d}\mathbf{x}\, \mathrm{d}\mathbf{x}' \int_0^\beta \mathrm{d}\tau\, \mathrm{d}\tau'\, \varphi(\mathbf{x},\tau)\cdot \mathbf{n}_s(\mathbf{x},\tau) \mathbf{n}_s(\mathbf{x}',\tau') \cdot \varphi(\mathbf{x}',\tau') \rangle_{S_0} } \ldots .$$

The Fourier transform of the order-parameter field is given by

$$\varphi(\mathbf{x},\tau) = T \sum_{\omega_n} \int \mathrm{d}\mathbf{q}\, \phi(\mathbf{q},\omega_n)\, e^{-i(\mathbf{q}\cdot\mathbf{x} - \omega_n \tau)} \, , \tag{44}$$

where ω_n is a Matsubara frequency, which is equal to $2n\pi/\beta$. Thus, the partition function in Fourier space is

$$Z = \int \mathrm{d}\phi(\mathbf{q},\omega_n)\, \mathrm{d}\phi^*(\mathbf{q},\omega_n) e^{-T\sum_{\omega_n} \int \mathrm{d}\mathbf{q} \left[(1 - 2u'\, \chi(\mathbf{q},\omega_n))\, |\phi(\mathbf{q},\omega_n)|^2 \right] + \frac{u}{2N} |\phi(\mathbf{q},\omega_n)|^4} \, ,$$

which considers the expansion up to the fourth cumulant. The reference-system dynamic susceptibility χ is given by

$$\chi(\mathbf{q},\omega_n) = \int \mathrm{d}\mathbf{x}'' \int_0^\beta \mathrm{d}\tau'' \, \langle \mathbf{n}_s(\mathbf{x},\tau) \cdot \mathbf{n}_s(\mathbf{x}',\tau') \rangle_{S_0} e^{-i(\mathbf{q}\cdot\mathbf{x}'' - \omega_n \tau'')} \, , \tag{45}$$

where $\mathbf{x}''$ is equal to $\mathbf{x} - \mathbf{x}'$, and τ'' is equal to $\tau - \tau'$. The reference ensemble consists of free fermions. Hence, the derivation of dynamic susceptibility (in appendix E below) is easy within the relevant limits of ferromagnetic quantum phase transition. Thus, the partition function of the Landau-Ginzburg-Wilson theory is equal to

$$\int \mathrm{d}\phi(\mathbf{q},\omega_n)\, \mathrm{d}\phi^*(\mathbf{q},\omega_n) e^{-T\sum_{\omega_n} \int \mathrm{d}\mathbf{q} \left[1 - 8u'\pi^2\alpha \left(\frac{3K_F}{2} - \frac{\mathbf{q}^2}{8K_F} - \frac{\pi|\omega_n|}{\mathbf{q}} \right) \right] |\phi(\mathbf{q},\omega_n)|^2 + \frac{u}{2N} |\phi(\mathbf{q},\omega_n)|^4} \, . \tag{46}$$

The distance from the critical point for this transition is defined as

$$r = 1 - 12\pi^2 u' \alpha K_F ,$$

which reproduces the Stoner criterion [64]. For r greater than 0, the system is in a paramagnetic phase and for r less than 0, the system is in a ferromagnetic phase. The order-parameter-modes damping coefficient γ in this transition is equal to $8\pi^3 u'\alpha/q$ and the microscopic length ξ_0 is equal to $u'\pi^2\alpha/K_F$. Thus, the Landau-Ginzburg-Wilson functional for ferromagnetic-paramagnetic quantum phase transition is

$$S = T\sum_{\omega_n}\int \mathrm{d}\mathbf{q}\,(\,r + \xi_0\mathbf{q}^2 + \gamma|\omega_n|\,)\,|\phi(\mathbf{q},\omega_n)|^2 + \frac{uT}{2N}\sum_{\omega_n}\int \mathrm{d}\mathbf{q}\,\phi^4(\mathbf{q},\omega_n)\;. \quad (47)$$

4.2.3. Landau-Ginzburg-Wilson functional for antiferromagnetic quantum phase transition. The derivation of the Landau-Ginzburg-Wilson functional for antiferromagnetic quantum phase transition is similar to that for the ferromagnetic quantum phase transition. The antiferromagnet-paramagnet phase transition is observed at a nonzero wave vector $\mathbf{Q}$ at which the dynamic susceptibility has a peak. Thus, the expansion of dynamic susceptibility in terms of $\mathbf{q}'$, which is equal to $\mathbf{q}-\mathbf{Q}$, and ω_n is necessary. This expansion yields the Landau-Ginzburg-Wilson functional:

$$S = T\sum_{\omega_n}\int \mathrm{d}\mathbf{q}'\,(\,r + \xi_0\mathbf{q}'^2 + \gamma|\omega_n|\,)\,|\phi(\mathbf{q}',\omega_n)|^2 + \frac{uT}{2N}\sum_{\omega_n}\int \mathrm{d}\mathbf{q}'\,\phi^4(\mathbf{q}',\omega_n)\;. \quad (48)$$

The Landau-Ginzburg-Wilson functional in equation (48) is for the phase transition without disorder. The disorder in this functional is introduced by making the distance from the critical point r, the damping coefficient γ, the microscopic length scale ξ_0, and the coefficient u random functions of spatial position.

4.2.4. Modifications to the Landau-Ginzburg-Wilson functional. Modifications to the Landau-Ginzburg-Wilson functional are necessary for application of the strong-disorder renormalization group method. The functional is expressed in discrete space because the strong-disorder renormalization group method is a real-space method. To make this modification, rotor variables[29] are introduced to

[29] A rotor is not observed in nature; it is a mathematical construction. It represents the effective degrees of freedom of the low-energy states of a small number of fermions with strong interactions.

represent the order-parameter average over a volume centered at a specific site[30]. The spatial gradient of the order-parameter field appears as an interaction J_{ij} between neighboring sites.

The second modification concerns the number of order parameter components N. Although the physical value of this number is 3, the strong-disorder renormalization group calculations are performed within the limit of large N. The fixed point of the strong-disorder renormalization group method is shown[31] identical for all N greater than 1. For a large N, the quartic term in equation (48) can be replaced by the length constraint on the order-parameter component at each site:

$$\left\langle |\varphi_j^k(\tau)|^2 \right\rangle = 1 \,, \tag{49}$$

where k represents the order-parameter component index. The Lagrange multiplier λ_i introduces this constraint in the Landau-Ginzburg-Wilson functional, which expresses the functional as

$$\begin{aligned} S =& T \sum_i \sum_{\omega_n} (r_i + \lambda_i + \gamma_i |\omega_n|) \, |\phi_i(\omega_n)|^2 \\ & - T \sum_{\langle i,j \rangle} \sum_{\omega_n} \phi_i(-\omega_n) \, J_{ij} \, \phi_j(\omega_n) \,. \end{aligned} \tag{50}$$

4.2.5. A single-site solution. The Landau-Ginzburg-Wilson functional for a single site is

$$S_{\text{single-site}} = T \sum_{\omega_n} (r + \lambda + \gamma |\omega_n|) \, |\phi(\omega_n)|^2 \,.$$

The Lagrange multiplier λ for a single site is given by the length constraint:

$$\left\langle |\varphi(\tau)|^2 \right\rangle = 1 \,. \tag{51}$$

Use of the Fourier transform (i.e., equation (44)) yields the length constraint in terms

[30] So far, the indices i and j have been used to represent spin states; henceforth, they will represent sites in the discrete space.

[31] See subsection 4.5.3.

of $\phi(\omega_m)$:

$$T^2 \sum_{\omega_m} \left\langle |\phi(\omega_m)|^2 \right\rangle = 1. \tag{52}$$

The order-parameter average is

$$\left\langle |\phi(\omega_m)|^2 \right\rangle = \frac{\int \mathrm{d}\phi(\omega_n)\, \mathrm{d}\phi^*(\omega_n)\, |\phi(\omega_m)|^2\, e^{-T\sum_{\omega_n}(r+\lambda+\gamma|\omega_n|)\,|\phi(\omega_n)|^2}}{\int \mathrm{d}\phi(\omega_n)\, \mathrm{d}\phi^*(\omega_n)\, e^{-T\sum_{\omega_n}(r+\lambda+\gamma|\omega_n|)\,|\phi(\omega_n)|^2}} .$$

Integrals in the above equation split for a frequency ω_m:

$$\frac{\int \mathrm{d}\phi(\omega_m)\, \mathrm{d}\phi^*(\omega_m)\, |\phi(\omega_m)|^2\, e^{-T(\epsilon+\gamma|\omega_m|)\,|\phi(\omega_m)|^2}}{\int \mathrm{d}\phi(\omega_m)\, \mathrm{d}\phi^*(\omega_m)\, e^{-T(\epsilon+\gamma|\omega_m|)\,|\phi(\omega_m)|^2}}$$
$$\times \frac{\int \mathrm{d}\phi(\omega_n)\, \mathrm{d}\phi^*(\omega_n)\, e^{-T\sum_{\omega_n\neq\omega_m}(\epsilon+\gamma|\omega_n|)\,|\phi(\omega_n)|^2}}{\int \mathrm{d}\phi(\omega_n)\, \mathrm{d}\phi^*(\omega_n)\, e^{-T\sum_{\omega_n\neq\omega_m}(\epsilon+\gamma|\omega_n|)\,|\phi(\omega_n)|^2}} ,$$

where ϵ is equal to $r+\lambda$. Use of equation (C.3) to solve the first term in this equation yields the order-parameter average:

$$\left\langle |\phi(\omega_m)|^2 \right\rangle = \frac{1}{T\,(\epsilon+\gamma|\omega_m|)} . \tag{53}$$

The single-site constraint from equations (52) and (53) is

$$T\sum_{\omega_m} \frac{1}{\epsilon+\gamma|\omega_m|} = 1 . \tag{54}$$

At absolute zero, the above summation can be transformed into an integral:

$$\frac{1}{2\pi}\int_{-\Lambda}^{\Lambda} \frac{\mathrm{d}\omega_m}{(\epsilon+\gamma|\omega_m|)} = 1 ,$$

where Λ is a microscopic cut-off frequency. Thus, the solution is $\ln\left(1+\frac{\gamma\Lambda}{\epsilon}\right) = \pi\gamma$. Because $\gamma\Lambda/\epsilon$ is much greater than 1, this equation yields the relationship between the effective distance from the critical point ϵ and the damping coefficient γ:

$$\epsilon = \gamma\Lambda e^{-\pi\gamma} . \tag{55}$$

4.3. APPLICATION OF THE STRONG-DISORDER RENORMALIZATION GROUP METHOD

Recursion relationships are derived here by applying the strong-disorder renormalization group method to the Landau-Ginzburg-Wilson functional (i.e., equation (50)) in a one-dimensional system[32]. They show changes in the coupling constants during the elimination process for degrees of freedom contributing to higher energies. The coupling constants, which are a local distance from the critical point ϵ_i and a bond J_{ij}, are the competing energies in the system. Following the steps outlined in subsection 3.2.1 for the strong-disorder renormalization group method, the largest local energy $\Omega = \max(\epsilon_i, J_{ij})$ is first identified. Of the two cases of Ω, the first to be discussed here is that of Ω equal to the effective distance from the critical point at site 2.

4.3.1. Decimation of a site. If ϵ_2 is much greater than J_{12} and J_{23}, the rotor ϕ_2 does not contribute to the order-parameter field. The large local energy, ϵ_2, inhibits polarization of this rotor. Hence, it is eliminated in the perturbation theory treatment, as shown in figure 4.5.

[32]The generalization of recursion relationships to higher dimensions is straight forward.

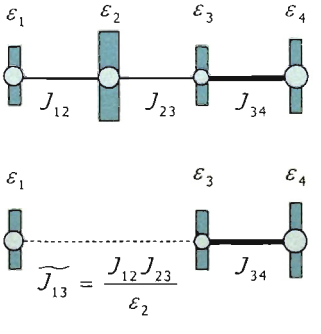

Figure 4.5. Decimation of a site for a large ϵ.

The partition function for the cluster of sites 1, 2, and 3 is

$$Z = \int \mathrm{d}\phi_1^*(\omega_n)\,\mathrm{d}\phi_1(\omega_n)\,\mathrm{d}\phi_2(\omega_n)\,\mathrm{d}\phi_2^*(\omega_n)\,\mathrm{d}\phi_3^*(\omega_n)\,\mathrm{d}\phi_3(\omega_n)\,e^{-(S_0+S_1)}\ ,$$

where

$$S_0 = T\sum_{\omega_n}\left(\epsilon_2 + \gamma_2|\omega_n|\right)|\phi_2(\omega_n)|^2$$

and

$$S_1 = -T\left[\sum_{\omega_n}\phi_1(-\omega_n)\,J_{12}\,\phi_2(\omega_n) + \sum_{\omega_n}\phi_2(-\omega_n)\,J_{23}\,\phi_3(\omega_n)\right]\ .$$

Elimination of the rotor ϕ_2 by carrying out Gaussian integral over $\phi_2(\omega_n)$ and $\phi_2^*(\omega_n)$ yields the partition function:

$$\tilde{Z} = \int \mathrm{d}\phi_1^*(\omega_n)\,\mathrm{d}\phi_1(\omega_n)\,\mathrm{d}\phi_3^*(\omega_n)\,\mathrm{d}\phi_3(\omega_n)\,e^{T\sum_{\omega_n}\phi_1(-\omega_n)\,\tilde{J}_{13}\,\phi_3(\omega_n)}\ ,$$

where sites 1 and 3 are connected by an effective interaction $\tilde{J}_{13}$. The method of cumulant expansion (i.e., equation (B.1)) is used to find this interaction. Thus,

$$\begin{aligned}-T\sum_{\omega_n}\phi_1(-\omega_n)\,\tilde{J}_{13}\phi_3(\omega_n) &= -\ln\left\langle e^{S_1}\right\rangle_0 \\ &= -\left\langle S_1\right\rangle_0 - \frac{1}{2}\left(\left\langle S_1^2\right\rangle_0 - \left\langle S_1\right\rangle_0^2\right) + O(S_1^3)\ , \qquad (56)\end{aligned}$$

where $\langle S_1\rangle_0$ implies the average of S_1 with respect to S_0. The first term of the expansion is

$$\begin{aligned}\left\langle S_1\right\rangle_0 = &\frac{-T\sum_{\omega_n}\phi_1(-\omega_n)\,J_{12}\int \mathrm{d}\phi_2(\omega_n)\,\mathrm{d}\phi_2^*(\omega_n)\,\phi_2(\omega_n)\,e^{-S_0}}{\int \mathrm{d}\phi_2(\omega_n)\,\mathrm{d}\phi_2^*(\omega_n)\,e^{-S_0}} \\ &- \frac{T\sum_{\omega_n}\phi_3(\omega_n)\,J_{23}\int \mathrm{d}\phi_2(\omega_n)\,\mathrm{d}\phi_2^*(\omega_n)\phi_2(-\omega_n)\,e^{-S_0}}{\int \mathrm{d}\phi_2(\omega_n)\,\mathrm{d}\phi_2^*(\omega_n)\,e^{-S_0}}\ .\end{aligned}$$

Because the integrals in numerators run from $-\infty$ to $+\infty$, they vanish due to symmetry. Therefore,

$$\langle S_1 \rangle_0 = 0. \tag{57}$$

Because

$$S_1^2 = T \sum_{\omega_n} |\phi_1(\omega_n)|^2 J_{12}^2 |\phi_2(\omega_n)|^2 + |\phi_2(\omega_n)|^2 J_{23}^2 |\phi_3(\omega_n)|^2 + 2\phi_1(-\omega_n) J_{12} J_{23} \phi_3(\omega_n) |\phi_2(\omega_n)|^2 ,$$

the average, $\langle S_1^2 \rangle_0$, in the second term of the expansion is

$$\langle S_1^2 \rangle_0 = \frac{T \sum_{\omega_n} |\phi_1(\omega_n)|^2 J_{12}^2 \int \mathrm{d}\phi_2(\omega_n)\, \mathrm{d}\phi_2^*(\omega_n)\, |\phi_2(\omega_n)|^2 e^{-S_0}}{\int \mathrm{d}\phi_2(\omega_n)\, \mathrm{d}\phi_2^*(\omega_n)\, e^{-S_0}} + \frac{T \sum_{\omega_n} |\phi_3(\omega_n)|^2 J_{23}^2 \int \mathrm{d}\phi_2(\omega_n)\, \mathrm{d}\phi_2^*(\omega_n)\, |\phi_2(\omega_n)|^2 e^{-S_0}}{\int \mathrm{d}\phi_2(\omega_n)\, \mathrm{d}\phi_2^*(\omega_n)\, e^{-S_0}} + \frac{2T \sum_{\omega_n} \phi_1(-\omega_n)\, J_{12} J_{23}\, \phi_3(\omega_n) \int \mathrm{d}\phi_2(\omega_n)\, \mathrm{d}\phi_2^*(\omega_n)\, |\phi_2(\omega_n)|^2 e^{-S_0}}{\int \mathrm{d}\phi_2(\omega_n)\, \mathrm{d}\phi_2^*(\omega_n)\, e^{-S_0}} .$$

Use of this result in equation (C.3) yields

$$\langle S_1^2 \rangle_0 = T \sum_{\omega_n} \left[\frac{J_{12}^2 |\phi_1(\omega_n)|^2}{\epsilon_2 + \gamma_2 |\omega_n|} + \frac{J_{23}^2 |\phi_3(\omega_n)|^2}{\epsilon_2 + \gamma_2 |\omega_n|} + \frac{2 J_{12} J_{23}\, \phi_1(-\omega_n) \phi_3(\omega_n)}{\epsilon_2 + \gamma_2 |\omega_n|} \right] . \tag{58}$$

The first two terms in this equation provide a subleading correction to ϵ_1 and ϵ_3. The last term gives the effective interaction between the rotors at sites 1 and 3, which were interacting with rotor ϕ_2. Its denominator can be simplified in the low frequency limit (i.e., $\gamma_2 |\omega_n| / \epsilon_2$ is much less than 1) as

$$\frac{1}{\epsilon_2 + \gamma_2 |\omega_n|} = \frac{1}{\epsilon_2} \left(1 - \frac{\gamma_2 |\omega_n|}{\epsilon_2} + \left(\frac{\gamma_2 |\omega_n|}{\epsilon_2} \right)^2 - .... \right) .$$

The denominator is then

$$\frac{1}{\epsilon_2 + \gamma_2 |\omega_n|} \approx \frac{1}{\epsilon_2} \tag{59}$$

in the low frequency limit. Thus,

$$\tilde{J}_{13} \approx \frac{J_{12}\, J_{23}}{\epsilon_2}\ , \tag{60}$$

which is derived by discarding higher-order cumulants in equation (56) and using equations (57), (58), and (59).

4.3.2. Decimation of a bond. If the largest local energy is the bond J_{23}, then J_{23} is much greater than ϵ_2 and ϵ_3 in a cluster of sites 2 and 3. Therefore, rotors ϕ_2 and ϕ_3 tend to be parallel and contribute to the order-parameter field as if there were only one rotor, $\tilde{\phi}_2$, as shown in figure 4.6. The functional of the cluster is

$$S = T\sum_{\omega_n} -\phi_2(-\omega_n)\, J_{23}\, \phi_3(\omega_n) + (\epsilon_2 + \gamma_2|\omega_n|)\, |\phi_2(\omega_n)|^2 + (\epsilon_3 + \gamma_3|\omega_n|)\, |\phi_3(\omega_n)|^2\ . \tag{61}$$

The mixed terms of rotors ϕ_2 and ϕ_3 in the functional are simplified by transforming the functional into the eigenbasis of ψ_+ and ψ_-. The matrix form of equation (61) is

$$S = T\sum_{\omega_n} \begin{pmatrix} \phi_2(-\omega_n) & \phi_3(-\omega_n) \end{pmatrix} \begin{pmatrix} \alpha_2 & -\frac{J_{23}}{2} \\ -\frac{J_{32}}{2} & \alpha_3 \end{pmatrix} \begin{pmatrix} \phi_2(\omega_n) \\ \phi_3(\omega_n) \end{pmatrix}\ ,$$

where α_2 is equal to $\epsilon_2 + \gamma_2|\omega_n|$ and α_3 is equal to $\epsilon_3 + \gamma_3|\omega_n|$.

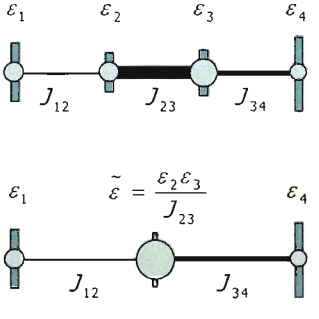

Figure 4.6. Decimation of a bond for a large J.

Eigenvalues and eigenvectors of above matrix are

$$\begin{aligned} E_+ =& \frac{(\alpha_2+\alpha_3)+\sqrt{(\alpha_2-\alpha_3)^2+J_{23}^2}}{2}\,, \\ E_- =& \frac{(\alpha_2+\alpha_3)-\sqrt{(\alpha_2-\alpha_3)^2+J_{23}^2}}{2} \end{aligned} \tag{62}$$

and

$$\begin{aligned} \psi_+ =& \cos\left(\frac{\theta}{2}\right)\phi_2(\omega_n)+\sin\left(\frac{\theta}{2}\right)\phi_3(\omega_n)\,, \\ \psi_- =& \sin\left(\frac{\theta}{2}\right)\phi_2(\omega_n)+\cos\left(\frac{\theta}{2}\right)\phi_3(\omega_n) \end{aligned} \tag{63}$$

respectively, where $\tan\theta$ is equal to $J_{23}/(\alpha_3-\alpha_2)$. Therefore, the functional (i.e., equation (61)) in the new basis is

$$S' = T\sum_{\omega_n} E_+|\psi_+(\omega_n)|^2 + E_-|\psi_-(\omega_n)|^2. \tag{64}$$

Expansion of equation (62) yields the energy eigenvalue E_-

$$E_- = \frac{\alpha_2+\alpha_3-J_{23}}{2} - \frac{(\alpha_2-\alpha_3)^2}{2J_{23}} + \ldots\,.$$

The higher order terms in above expansion can be discarded for J_{23} much greater than ϵ_2 and ϵ_3. Thus, the damping coefficient and the effective distance from critical point are

$$\tilde{\gamma} = \gamma_2 + \gamma_3$$

and

$$\tilde{\epsilon} = \epsilon_2 + \epsilon_3 - J_{23}$$

respectively. Definition of two variables, $X_1 = \epsilon_2 - \frac{J_{23}}{2}$ and $X_2 = \epsilon_3 - \frac{J_{23}}{2}$, yields the

product of ϵ_2 and ϵ_3:

$$\epsilon_2\epsilon_3 = X_1X_2 + \frac{\tilde{\epsilon}J_{23}}{2} + \frac{J_{23}^2}{4} .$$

Because the term X_1X_2 is much less than $\tilde{\epsilon}$, the effective distance from the critical point is

$$\tilde{\epsilon} \approx 2\frac{\epsilon_2\epsilon_3 - J_{23}^2/4}{J_{23}} . \tag{65}$$

Appendix F implements the length constraint at sites 2 and 3 to reduce equation (65) to

$$\tilde{\epsilon} \approx 2\frac{\gamma_2\gamma_3\Lambda^2 e^{-\pi(\gamma_2+\gamma_3)}}{J_{23}} . \tag{66}$$

The right hand side of this equation is a product of the single-site constraint (i.e., equation (55)) at sites 2 and 3. Hence, the effective distance from the critical point is

$$\tilde{\epsilon} \approx 2\frac{\epsilon_2^0\epsilon_3^0}{J_{23}} , \tag{67}$$

where ϵ_2^0 is equal to $\gamma_2\Lambda e^{-\pi\gamma_2}$ and ϵ_3^0 is equal to $\gamma_3\Lambda e^{-\pi\gamma_3}$ [65, 66]. Though this recursion relationship differs from equation (32) by a factor of 2, $\tilde{\epsilon}$ is always less than ϵ_2^0 and ϵ_3^0 if J_{23} is much greater than ϵ_2^0 and ϵ_3^0. Thus, the general form of recursion relationships for the decimation of sites and bonds is

$$\tilde{J}_{i-1,i+1} \approx \frac{J_{i-1,i}\, J_{i,i+1}}{\epsilon_i}$$
$$\tilde{\epsilon} \approx 2\frac{\epsilon_i^0\epsilon_{i+1}^0}{J_{i,i+1}} .$$

The result of above decimation procedures is removal of a site and reduction in the maximum energy scale Ω. These decimations are iterated ad infinitum.

4.4. FLOW EQUATIONS AND THEIR SOLUTION

Derivation of flow equations, which result from the above recursion relationships, is possible only for a one-dimensional system. Decimation of a site and decimation of a bond are statistically independent, therefore, flow equations are derived for the probability distributions of variables J and ϵ, which are P and R respectively.

4.4.1. Flow equations. The recursion relationships are multiplicative. Hence, formulation of flow equations is convenient in terms of logarithmic variables, which are

$$\zeta = \ln\left(\frac{\Omega}{J}\right) \ , \ \beta = \ln\left(\frac{\Omega}{\epsilon}\right) \ , \text{and } \Gamma = \ln\left(\frac{\Omega_I}{\Omega}\right) \ , \tag{68}$$

where Ω_I is the system's initial energy scale, which is reduced in the renormalization procedure. The energy scale Ω is reduced to a final energy scale $\Omega - \mathrm{d}\Omega$ during elimination of all rotors and bonds for which $\Omega > \epsilon > \Omega - \mathrm{d}\Omega$ and $\Omega > J > \Omega - \mathrm{d}\Omega$. Thus, the energy scale changes from Γ to $\Gamma + \mathrm{d}\Gamma$ during decimations for which recursion relationships in equations (60) and (67) are redefined as $\tilde{\zeta} = \zeta_2 + \zeta_3$ and $\tilde{\beta} = \beta_2 + \beta_3$ respectively. The following discusses variations in the probability distribution functions due to these recursion relationships. The probability distribution function $P(\zeta, \Gamma)$ of bonds varies due to decimation of sites:

$$\begin{aligned} P(\tilde{\zeta}, \Gamma + \mathrm{d}\Gamma) = \Big\{ & P(\zeta,\Gamma) - \mathrm{d}\Gamma R(0,\Gamma)\, P(\zeta,\Gamma) \int \mathrm{d}\zeta_2\, P(\zeta_2,\Gamma) \\ & - \mathrm{d}\Gamma R(0,\Gamma)\, P(\zeta,\Gamma) \int \mathrm{d}\zeta_3\, P(\zeta_3,\Gamma) \\ & + \mathrm{d}\Gamma\, R(0,\Gamma) \int \mathrm{d}\zeta_2 \int \mathrm{d}\zeta_3\, P(\zeta_2,\Gamma) P(\zeta_3,\Gamma) \delta(\tilde{\zeta} - \zeta_2 - \zeta_3) \Big\} \\ & \times \left[1 - \mathrm{d}\Gamma(P(0,\Gamma) + R(0,\Gamma))\right]^{-1} , \end{aligned} \tag{69}$$

where $P(\tilde{\zeta}, \Gamma + \mathrm{d}\Gamma)$ and $P(\zeta, \Gamma)$ are the respective probability distribution functions after and before the decimation. The term $R(0, \Gamma)$ represents the probability distribution function at $\epsilon_2 = \Omega$. The second and third terms in the curly brackets come

from the elimination of J_{12} and J_{23} respectively. The fourth term in the curly brackets comes from the addition of bond $\tilde{J}_{13}$. The multiplying term is for normalization of distribution functions.

Because $\mathrm{d}\Gamma(P(0,\Gamma)+R(0,\Gamma))$ is much less than 1, the normalizing factor is

$$[1-\mathrm{d}\Gamma(P(0,\Gamma)+R(0,\Gamma))]^{-1}\approx[1+\mathrm{d}\Gamma(P(0,\Gamma)+R(0,\Gamma))]\ .$$

Because $\int \mathrm{d}\zeta_2 P(\zeta_2,\Gamma)$ and $\int \mathrm{d}\zeta_3 P(\zeta_3,\Gamma)$ are both equal to 1, equation (69) can be reduced to

$$\begin{aligned}P(\tilde{\zeta},\Gamma+\mathrm{d}\Gamma)=\Big\{&P(\zeta,\Gamma)-2\mathrm{d}\Gamma\,R(0,\Gamma)\,P(\zeta,\Gamma)\\&+\mathrm{d}\Gamma\,R(0,\Gamma)\int \mathrm{d}\zeta_2\,P(\zeta_2,\Gamma)P(\tilde{\zeta}-\zeta_2,\Gamma)\Big\}\\&\times\left[1+\mathrm{d}\Gamma(P(0,\Gamma)+R(0,\Gamma))\right]\ .\end{aligned}$$

The higher order terms of $\mathrm{d}\Gamma$ in above product are discarded because they are small. Hence, the above equation can be simplified as

$$\begin{aligned}P(\tilde{\zeta},\Gamma+\mathrm{d}\Gamma)=&P(\zeta,\Gamma)-2\mathrm{d}\Gamma\,R(0,\Gamma)P(\zeta,\Gamma)\\&+\mathrm{d}\Gamma\,R(0,\Gamma)[P(\zeta_2)*P(\tilde{\zeta}-\zeta_2)]\\&+\mathrm{d}\Gamma\,P(0,\Gamma)P(\zeta,\Gamma)+\mathrm{d}\Gamma\,R(0,\Gamma)P(\zeta,\Gamma),\end{aligned}\tag{70}$$

where $P(\zeta_2)*P(\tilde{\zeta}-\zeta_2)$ is the convolution of $P(\zeta_2,\Gamma)$ and $P(\tilde{\zeta}-\zeta_2,\Gamma)$. Because

$$\begin{aligned}\mathrm{d}P=&P(\tilde{\zeta},\Gamma+\mathrm{d}\Gamma)-P(\zeta,\Gamma)\\=&\left(\frac{\partial P}{\partial\Gamma}\mathrm{d}\Gamma+\frac{\partial P}{\partial\zeta}\mathrm{d}\zeta\right)=\left(\frac{\partial P}{\partial\Gamma}-\frac{\partial P}{\partial\zeta}\right)\mathrm{d}\Gamma\ ,\end{aligned}$$

equation (70) can be reduced to

$$\frac{\partial P}{\partial\Gamma}=\frac{\partial P}{\partial\zeta}-R(0,\Gamma)P(\zeta,\Gamma)+R(0,\Gamma)[P(\zeta_2)*P(\tilde{\zeta}-\zeta_2)]+P(0,\Gamma)P(\zeta,\Gamma)\ .\tag{71}$$

Thus, equation (71) gives the variation in the probability distribution, $P(\zeta, \Gamma)$, for decimation of sites.

Variation in the probability distribution function $R(\beta, \Gamma)$ due to decimation of bonds is

$$\begin{aligned} R(\tilde{\beta}, \Gamma + \mathrm{d}\Gamma) = & \Big\{ R(\beta, \Gamma) - \mathrm{d}\Gamma\, P(0, \Gamma) R(\beta, \Gamma) \int \mathrm{d}\beta_2\, R(\beta_2, \Gamma) \\ & - \mathrm{d}\Gamma\, P(0, \Gamma) R(\beta, \Gamma) \int \mathrm{d}\beta_3\, R(\beta_3, \Gamma) \\ & + \mathrm{d}\Gamma\, P(0, \Gamma) \int \mathrm{d}\beta_2 \int \mathrm{d}\beta_3\, R(\beta_2, \Gamma) R(\beta_3, \Gamma) \delta(\tilde{\beta} - \beta_2 - \beta_3) \Big\} \\ & \times [1 - \mathrm{d}\Gamma(P(0, \Gamma) + R(0, \Gamma))]^{-1} \ , \end{aligned} \tag{72}$$

where $R(\tilde{\beta}, \Gamma + \mathrm{d}\Gamma)$ and $R(\beta, \Gamma)$ are the respective probability distribution functions after and before the decimation. The term $P(0, \Gamma)$ represents the probability distribution function at $J_{23} = \Omega$. The second, third and fourth term on the right hand side come from the elimination of ϵ_2^0, ϵ_3^0 and the addition of $\tilde{\epsilon}$ respectively. The last term is due to normalization of distribution functions.

In equation (72), $\int \mathrm{d}\beta_2 R(\beta_2, \Gamma)$ and $\int \mathrm{d}\beta_3 R(\beta_3, \Gamma)$ are both equal to 1. Using approximations similar to that used to obtain equation (70), equation (72) reduces to

$$\begin{aligned} R(\tilde{\beta}, \Gamma + \mathrm{d}\Gamma) = & R(\beta, \Gamma) - 2\mathrm{d}\Gamma P(0, \Gamma) R(\beta, \Gamma) \\ & + \mathrm{d}\Gamma P(0, \Gamma)[R(\beta_2) * R(\tilde{\beta} - \beta_2)] \\ & + \mathrm{d}\Gamma R(0, \Gamma) R(\beta, \Gamma) + \mathrm{d}\Gamma P(0, \Gamma) R(\beta, \Gamma). \end{aligned} \tag{73}$$

Because

$$\mathrm{d}R = R(\tilde{\beta}, \Gamma + \mathrm{d}\Gamma) - R(\beta, \Gamma) = \left(\frac{\partial R}{\partial \Gamma} - \frac{\partial R}{\partial \beta} \right) \mathrm{d}\Gamma,$$

equation (73) is reduced to

$$\frac{\partial R}{\partial \Gamma} = \frac{\partial R}{\partial \beta} - P(0, \Gamma) R(\beta, \Gamma) + P(0, \Gamma)[R(\beta_2) * R(\tilde{\beta} - \beta_2)] + R(0, \Gamma) R(\beta, \Gamma). \tag{74}$$

Thus, equation (74) gives the variation in the probability distribution $R(\beta, \Gamma)$ for the decimation of bonds.

4.4.2. Probability distribution functions at and near the critical point. When the system goes to paramagnetic phase under iterations of recursion relationships, variables J become small compared to variables ϵ. Hence, the process of eliminating rotors prevents formation of a large cluster. On the other hand, if the system goes to magnetic phase, then variables ϵ become small compared to J. Thus, the process of combining two rotors leads to formation of a large cluster. At the critical point, the probability distributions of two variables are equal because the system is in neither phase.

The following discusses the functional forms of the probability distribution functions at the critical point. These functions are assumed[33] to be

$$P(\zeta, \Gamma) = P_0(\Gamma) e^{-P_0(\Gamma)\zeta} \text{ and } R(\beta, \Gamma) = R_0(\Gamma) e^{-R_0(\Gamma)\beta} .$$

Substituting these trial functions in the flow equations (71) and (74) yields functional forms of $P_0(\Gamma)$ and $R_0(\Gamma)$, which in turn give the probability distribution functions at the critical point. The following illustrates the derivation of $P_0(\Gamma)$. Substitution of trial functions in equation (71) yields:

$$P(\zeta, \Gamma) \frac{\partial P_0(\Gamma)}{\partial \Gamma} \left(\frac{1}{P_0(\Gamma)} - \zeta \right) = -P_0(\Gamma) P(\zeta, \Gamma) - R_0(\Gamma) P(\zeta, \Gamma) + R_0(\Gamma) P_0(\Gamma) \zeta P(\zeta, \Gamma) + P_0(\Gamma) P(\zeta, \Gamma) ,$$

where $P(\zeta_2) * P(\tilde{\zeta} - \zeta_2) \equiv P_0(\Gamma) \zeta P(\zeta, \Gamma)$, $R(0, \Gamma) = R_0(\Gamma) = P_0(\Gamma)$ and $P(0, \Gamma) = P_0(\Gamma)$. Thus,

$$\frac{\mathrm{d}P}{\mathrm{d}\Gamma} = -P_0^2(\Gamma) ,$$

which is satisfied by $P_0(\Gamma) = 1/\Gamma$. Likewise, the use of trial functions in equation (74) yields $R_0(\Gamma) = 1/\Gamma$. Hence, the probability distribution functions at the critical

[33] A rigorous derivation of probability distribution functions can be found in [41] and the references therein.

point are

$$P(\zeta,\Gamma)=\frac{e^{-\frac{\zeta}{\Gamma}}}{\Gamma}\text{ and }R(\beta,\Gamma)=\frac{e^{-\frac{\beta}{\Gamma}}}{\Gamma}\,. \tag{75}$$

Therefore, because the energy scale Ω tends to 0, the logarithmic variable Γ diverges; consequently, both distribution functions become broad. In this situation, the approximate recursion relationships become exact because removal of a rotor or a bond corresponds to a small fractional change in the energy scale.

For the system away from the critical point, the distance from that point is given by

$$r=\frac{\overline{\ln\epsilon}-\overline{\ln J}}{\mathrm{var}(\ln\epsilon)+\mathrm{var}(\ln J)}\,. \tag{76}$$

Invariance of r under the renormalization procedure justifies this definition. The system is in paramagnetic phase if r greater than 0 and in magnetic phase if r is less than 0. The solutions [41] of equations (71) and (74) in the limit $r\to 0$ and $\Gamma\to\infty$ are

$$\begin{aligned}P(\zeta,\Gamma)&=\frac{2r}{e^{2r\Gamma}-1}\exp\left(-\frac{2\zeta r}{e^{2r\Gamma}-1}\right)\text{ and}\\ R(\beta,\Gamma)&=\frac{-2r}{e^{-2r\Gamma}-1}\exp\left(\frac{2\beta r}{e^{-2r\Gamma}-1}\right)\,,\end{aligned} \tag{77}$$

which give the probability distribution functions near the critical point.

4.4.3. Scaling forms of number density and moment. The number density n_Γ is the number of clusters surviving at energy scale Γ. The bonds and sites for which the respective ζ and β are approximately equal to 0 are removed when the energy scale changes from Γ to $\Gamma+\mathrm{d}\Gamma$. If $n_{\mathrm{S}}(\zeta,\Gamma)$ and $n_{\mathrm{B}}(\beta,\Gamma)$ are the number of sites and bonds at energy scale Γ, then the number density at this scale varies as

$$\frac{\mathrm{d}n_\Gamma}{\mathrm{d}\Gamma}=-[P_0(\Gamma)+R_0(\Gamma)]n_\Gamma\,,$$

where $P_0(\Gamma)$ is equal to $n_{\mathrm{S}}(0,\Gamma)/n_\Gamma$ and $R_0(\Gamma)$ is equal to $n_{\mathrm{B}}(0,\Gamma)/n_\Gamma$. The solution

of this equation at the critical point is

$$n_\Gamma \sim 1/\Gamma^2 ,$$

which is the scaling form of number density at that point for a one-dimensional system. The number density relates the length to the energy scale of the system. Because typical cluster length L is approximately equal to $1/n_\Gamma$, the above scaling form yields

$$L^{1/2} = \ln\left(\frac{\Omega_I}{\Omega}\right) , \tag{78}$$

which is the length scale of a surviving cluster given by equation (34). Thus, the critical exponent ψ, defined in equation (35), is equal to 1/2.

For the system at some distance from the critical point, Γ scales as $1/r$, where r is the distance from the critical point given by equation (76). Thus, from the relationship between the length of the surviving cluster and the energy scale, the correlation length of the system is given by

$$\xi \sim 1/r^2 .$$

Hence, the correlation length critical exponent ν is equal to 2.

The analysis thus far is for a one-dimensional system. The strong-disorder renormalization group method cannot give a closed-form solution for higher dimensions because the lattice topology changes under the recursion relationships. However, the scaling forms in one dimension can be generalized to higher dimensions. Thus, the scaling form of number density in d dimension is

$$n_\Gamma(r) = \Gamma^{-d/\psi}\mathcal{N}(r^{\nu\psi}\Gamma) . \tag{79}$$

In the limit $x \to \infty$, the scaling function $\mathcal{N}(x)$ is approximately equal to $x^{d/\psi}e^{-cdx}$, where c is a constant. The scaling function is constant in the limit $x \to 0$. Thus, in the Griffiths paramagnetic region (where r is greater than 0), the number density is $n_\Gamma \sim r^{d\nu}e^{-\Gamma d/z}$, where the dynamical critical exponent z is equal to $r^{-\nu\psi}$.

The moment of a rotor formed by combining two rotors is equal to the sum of the moments of those rotors. Thus, the exact solution [41] in one dimension for typical moment of the cluster at the critical point is

$$\mu_\Gamma(r) = \Gamma^\phi \ ,$$

where ϕ is equal to $(1+\sqrt{5})/2$. This scaling form of the typical moment in one dimension can be generalized to a higher dimension as

$$\mu_\Gamma(r) = \Gamma^\phi \mathcal{M}(r^{\nu\psi}\Gamma) \ . \tag{80}$$

The scaling function $\mathcal{M}(x)$ is approximately equal to $x^{1-\phi}$ in the limit $x \to \infty$, and it is constant in the limit $x \to 0$. Thus, the typical moment of the cluster μ_Γ varies as $r^{\nu\psi(1-\phi)}\Gamma$ in this region. The scaling forms of number density and moment are used to find observable quantities as discussed below in section 4.5.

4.5. OBSERVABLE QUANTITIES

Thermodynamically observable quantities at some non-zero temperature T are calculated by applying the strong-disorder renormalization group method up to a finite energy scale equal to T. The remaining clusters present at that stage in the renormalization group are nearly independent because their interaction energies are much smaller than the thermal energy; consequently, each cluster contributes individually to the observed quantities. Therefore, the following first evaluates observed quantities of a cluster.

4.5.1. Observable quantities of a cluster. The Landau-Ginzburg-Wilson functional of a cluster is

$$S = T\sum_{\omega_n}\left[(\epsilon+\gamma|\omega_n|)\,|\phi(\omega_n)|^2 - \mathrm{H}(-\omega_n)\phi(\omega_n)\right] \ ,$$

where $\mathrm{H}(\omega_n)$ is a source field conjugate to the order parameter. Hence, the partition

function of the cluster is

$$Z \approx \frac{1}{2T\sum_{\omega_n}(\epsilon+\gamma|\omega_n|)} \exp\left(\frac{T\sum_{\omega_n} \mathrm{H}^2(\omega_n)}{4\sum_{\omega_n}(\epsilon+\gamma|\omega_n|)}\right) ;$$

therefore, the dynamic susceptibility is

$$\chi = \frac{\partial^2 \ln Z}{\partial \mathrm{H}(\omega_n)\partial \mathrm{H}(-\omega_n)} \approx \sum_{\omega_n} \frac{T}{(\epsilon+\gamma|\omega_n|)} . \tag{81}$$

The susceptibility at finite temperature is derived from the single-site constraint (i.e., equation (54)). At a non-zero temperature, the zero frequency term is treated separately. Hence, the constraint is

$$\frac{T}{\epsilon} + \frac{1}{\pi}\int_0^{\Lambda} \frac{\mathrm{d}\omega_n}{(\epsilon+\gamma|\omega_n|)} = 1 .$$

The solution of this equation is

$$\frac{T}{\epsilon} + \frac{1}{\pi\gamma}\ln\left(1+\frac{\gamma\Lambda}{\epsilon}\right) = 1 .$$

It is simplified in the two limiting cases. In the first case, temperature is much smaller than ϵ_0 (i.e., $\gamma T << \epsilon_0$, where ϵ_0 is given by equation (55)). If ϵ is equal to $\epsilon_0 + \delta$, where δ is a small correction due to temperature, then the above solution can be reduced to

$$\frac{T}{\epsilon_0} + \frac{1}{\pi\gamma}\ln\left(\frac{\gamma\Lambda}{\epsilon_0}\right) - \frac{\delta}{\pi\gamma\epsilon_0} = 1 . \tag{82}$$

Because $1/\pi\gamma \ln\left(\frac{\gamma\Lambda}{\epsilon_0}\right)$ is equal to 1, the small correction δ is equal to $\pi\gamma T$.

In the second case, temperature is much larger than ϵ_0 (i.e., $\gamma T >> \epsilon_0$). In this limit, the logarithmic term is very small; consequently, ϵ is equal to T. Thus,

$$\epsilon = \begin{cases} \epsilon_0 + \pi\gamma T & \text{if} \quad \gamma T << \epsilon_0 . \\ T & \text{if} \quad \gamma T >> \epsilon_0 \end{cases}$$

The order parameter represents a cluster of moment μ, and its contribution to

uniform order-parameter susceptibility is proportional to μ^2. Moreover, its contribution to local susceptibility is proportional to μ. Therefore, in the above two limiting cases, uniform and local susceptibilities of a cluster are given by

$$\chi_{\text{cluster}} = \begin{cases} \mu^2/\epsilon & \text{if} \quad \gamma T << \epsilon \\ \mu^2/T & \text{if} \quad \gamma T >> \epsilon \end{cases} \tag{83}$$

and

$$\chi_{\text{cluster-loc}} = \begin{cases} \mu/\epsilon & \text{if} \quad \gamma T << \epsilon \\ \mu/T & \text{if} \quad \gamma T >> \epsilon \end{cases} \tag{84}$$

respectively. The dynamic susceptibility (i.e., equation (81)) of a cluster at absolute zero is

$$\chi_{\text{cluster-dynamic}} = \frac{\mu^2}{(\epsilon + \gamma|\omega_n|\,)} \; ;$$

likewise, the dynamic local susceptibility of a cluster is

$$\chi_{\text{cluster-dynamic-loc}} = \frac{\mu}{(\epsilon + \gamma|\omega_n|\,)} \; .$$

The Wick rotation[34] $i\omega_n \rightarrow \omega + i\delta$, where δ is very small, gives the above susceptibilities in real frequencies as

$$\chi_{\text{cluster-dynamic}} = \frac{\mu^2}{(\epsilon - i\gamma\omega)} \quad \text{and} \quad \chi_{\text{cluster-dynamic-loc}} = \frac{\mu}{(\epsilon - i\gamma\omega)} \; .$$

Thus,

$$\text{Im}\ \chi_{\text{cluster-dynamic}} = \frac{\gamma\mu^2\omega}{(\epsilon^2 + \gamma^2\omega^2)} \quad \text{and} \quad \text{Im}\ \chi_{\text{cluster-dynamic-loc}} = \frac{\gamma\mu\omega}{(\epsilon^2 + \gamma^2\omega^2)} \; .$$

4.5.2. Observable quantities of the system. The following calculates observable quantities of the system by summing all surviving clusters. The renormalization group technique is carried out to energy scale Ω, which is equal to T, to find

[34]The term $-i\gamma\omega$ in the denominator of $\chi_{\text{cluster-dynamic}}$ is a result of Wick rotation carried out before expading the logarithmic term in equation (E.3).

the uniform susceptibility at temperature T. Under this condition, the logarithmic variable Γ is equal to $\ln(\Omega_I/T)$. Equations (79), (80), and (83) yield the scaling form of the uniform susceptibility:

$$\chi = \frac{1}{T} n_\Gamma(r) \mu_\Gamma^2(r) \ ,$$

i.e.,

$$\chi = \frac{1}{T} \left[\ln\left(\frac{\Omega_I}{T}\right) \right]^{2\phi - d/\psi} \mathcal{N}(r^{\nu\psi} \ln(\Omega_I/T)) \mathcal{M}^2(r^{\nu\psi} \ln(\Omega_I/T)) \ . \tag{85}$$

Therefore, the uniform susceptibility at the critical point (where r is equal to 0) is

$$\chi \sim \frac{1}{T} \left[\ln\left(\frac{\Omega_I}{T}\right) \right]^{2\phi - d/\psi} \ ,$$

and in the Griffiths paramagnetic region it is

$$\chi \sim T^{d/z-1} r^{\nu d + 2\nu\psi(1-\phi)} \left[\ln\left(\frac{\Omega_I}{T}\right) \right]^2 \ .$$

The scaling form of uniform susceptibility determines the shape of the phase boundary near the critical point. The scaling function of equation (85) has a singularity at a finite temperature critical point for a constant critical value of its argument, i.e.,

$$r^{\nu\psi} \ln\left(\frac{\Omega_I}{T_c}\right) = c \ .$$

Thus, the shape of the phase boundary near the critical point is

$$T_c = \exp(-c\, r^{-\nu\psi}) \ , \tag{86}$$

as shown in figure (4.7). The shape of the phase boundary agrees qualitatively with that of $CePd_{1-x}Rh_x$ in figure (4.1).

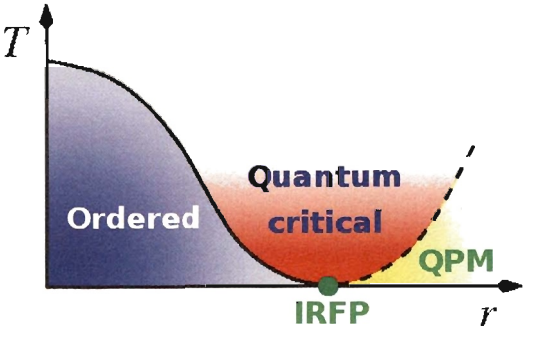

Figure 4.7. Phase diagram in the vicinity of an infinite randomness fixed point (IRFP). The shape of the phase boundary near the infinite randomness critical point is given by equation (86). The Griffiths paramagnetic region is represented by the quantum paramagnet (QPM). (Reprinted figure from Josè A. Hoyos, Chetan Kotabage, and Thomas Vojta , Physical Review Letters, 99, 230601 (2007). Copyright (2007) by the American Physical Society.)

The scaling form of the local susceptibility,

$$\chi_{\rm loc} = \frac{n_\Gamma(r)\mu_\Gamma(r)}{T} \ ,$$

i.e.,

$$\chi_{\rm loc} = \frac{1}{T}\left[\ln\left(\frac{\Omega_I}{T}\right)\right]^{\phi-d/\psi} \mathcal{N}(r^{\nu\psi}\ln(\Omega_I/T))\mathcal{M}(r^{\nu\psi}\ln(\Omega_I/T)) \ , \tag{87}$$

is obtained from equations (79), (80), and (84). Thus, the local susceptibility at the critical point and in the Griffiths paramagnetic region is

$$\chi_{\rm loc} \sim \frac{1}{T}\left[\ln\left(\frac{\Omega_I}{T}\right)\right]^{\phi-d/\psi}$$

and

$$\chi_{\rm loc} \sim T^{d/z-1} r^{\nu d+\nu\psi(1-\phi)} \ln\left(\frac{\Omega_I}{T}\right)$$

respectively.

The energy contribution of the clusters is found by summing the energies of all clusters. Therefore,

$$\Delta E = T n_T(r) = T \left[\ln \left(\frac{\Omega_I}{T} \right) \right]^{-d/\psi} \mathcal{N}(r^{\nu\psi} \ln(\Omega_I/T)) \; .$$

Thus, the specific heat is

$$C \sim (\ln(\Omega_I/T))^{-d/\psi}$$

at the critical point and

$$C \sim r^{\nu d} T^{d/z}$$

in the Griffiths paramagnetic region.

The low-temperature order parameter dependence on the conjugate field is calculated by applying the strong-disorder method down to energy Ω_{H}, which is equal to $\mu\mathrm{H}$. Clusters of energy ϵ (which is much greater than Ω_{H}) are decimated; hence, they do not contribute to the order parameter. But clusters of energy much less than Ω_{H} are polarized; therefore, they do contribute to the order parameter. The scaling form of the order parameter is

$$m = n_{\Omega_{\mathrm{H}}}(r) \mu_{\Omega_{\mathrm{H}}}(r) \; ,$$

i.e.,

$$m = \left[\ln \left(\frac{\Omega_I}{\Omega_{\mathrm{H}}} \right) \right]^{\phi - d/\psi} \mathcal{N}(r^{\nu\psi} \ln(\Omega_I/\Omega_{\mathrm{H}})) \mathcal{M}(r^{\nu\psi} \ln(\Omega_I/\Omega_{\mathrm{H}})) \; . \tag{88}$$

At the critical point (where r is equal to 0), the order parameter is

$$m \sim \left[\ln \left(\frac{\Omega_I}{\mathrm{H}} \right) \right]^{\phi - d/\psi} \; .$$

If this relationship is compared with the definition of exponent δ

$$m \sim \mathrm{H}^{1/\delta},$$

then δ is formally infinity. This order parameter has a correction of

$$-\left[\ln\left(\left[\ln\left(\frac{\Omega_I}{\mathrm{H}}\right)\right]^{\phi}\right)\right]^{\phi-d/\psi} , \tag{89}$$

which comes from the scaling form of the moment (i.e., equation (80)). The order parameter in the Griffiths paramagnetic region is

$$m = \mathrm{H}^{d/z} r^{d\nu+\nu\psi(1-\phi)(1+d/z)} \left[\ln(\Omega/\mathrm{H})\right]^{1+d/z} .$$

The scaling form of zero-temperature dynamic susceptibility at an external frequency ω and energy Ω_ω (which is equal to $\gamma\mu\omega$) is

$$\mathrm{Im}\,\chi = \frac{1}{\gamma\omega}\left[\ln\left(\Omega_I/\gamma\omega\right)\right]^{\phi-d/\psi} \mathcal{N}(r^{\nu\psi}\ln(\Omega_I/\gamma\omega))\mathcal{M}(r^{\nu\psi}\ln(\Omega_I/\gamma\omega)) ,$$

where γ is the damping coefficient of a single cluster. If the above correction (i.e., equation (89)) to the scaling form is discarded, then the dynamic susceptibility is

$$\mathrm{Im}\,\chi \sim \frac{1}{\gamma\omega}\left[\ln\left(\Omega_I/\gamma\omega\right)\right]^{\phi-d/\psi}$$

at the critical point. In the Griffiths paramagnetic region, the dynamic susceptibility is

$$\mathrm{Im}\,\chi \sim (\gamma\omega)^{d/z-1} r^{d\nu+\nu\psi(1-\phi)(1+d/z)} \left[\ln(\Omega/\gamma\omega)\right]^{1+d/z} .$$

The scaling form of local susceptibility is

$$\mathrm{Im}\,\chi_{\mathrm{loc}} = \frac{1}{\gamma\omega}\left[\ln(\Omega_I/\gamma\omega)\right]^{-d/\psi} \mathcal{N}(r^{\nu\psi}\ln(\Omega_I/\gamma\omega)) .$$

Thus, the local susceptibility is

$$\mathrm{Im}\,\chi_{\mathrm{loc}} \sim \frac{\left[\ln(\Omega_I/\gamma\omega)\right]^{-d/\psi}}{\gamma\omega}$$

at the critical point and

$$\mathrm{Im}\,\chi_{\mathrm{loc}} \sim (\gamma\omega)^{1-d/z}\, r^{d\nu+\nu\psi(1-\phi)d/z}\,[\ln(\Omega/\gamma\omega)]^{d/z}$$

in the Griffiths region.

4.5.3. Observable quantities for all N greater than 1. The observable quantities calculated above are for a large number of order parameter components, i.e., for the large N. To show that these results are valid for all N greater than 1 (i.e., for all continuous-symmetry cases), the recursion relationship for decimation of a site (i.e., equation (60)) and a bond (i.e., equation (67)) are considered.

Equation (60) for decimation of a site is derived from the second-order perturbation theory and is therefore valid for all N including the case of $N = 1$. The other recursion relationship in equation (67) for decimation of a bond combines two rotors. Previous research [67] has shown that for all continuous-symmetry cases of N greater than 1, the effective distance from the critical point ϵ is

$$\epsilon = e^{-c\mu}\,,$$

where c is a constant and μ is the moment of the cluster. The exponential relationship between ϵ and μ and this recursion relationship fulfill the condition that the moment of cluster formed by combining two rotors is equal to the sum of the moments of those rotors. Thus, this recursion relationship is valid for all N greater than 1. Therefore, the observable quantities found at and near the critical point for these recursion relationships are valid for all continuous-symmetry cases with N greater than 1.

Chapter 6 below summarizes the results obtained for observable quantities and compares them with conventional critical behavior and experiments.

5. SUPEROHMIC DAMPING IN QUANTUM PHASE TRANSITIONS

Chapter 4 considered the problem of a quantum phase transition in the presence of ohmic damping. This chapter considers a generalization of such a problem in which ohmic damping is replaced by superohmic damping. The motivation here is to investigate the changes in the characteristics of infinite randomness critical point when the damping gets weaker.

5.1. THE LANDAU-GINZBURG-WILSON FUNCTIONAL

The Landau-Ginzburg-Wilson functional derived in subsection 4.2.4 (i.e., equation (50)) can be generalized to

$$\begin{aligned} S =& T \sum_{i} \sum_{\omega_n} \left(r_i + \lambda_i + \gamma_i |\omega_n|^{2/z_0} \right) |\phi_i(\omega_n)|^2 \\ & - T \sum_{\langle i,j \rangle} \sum_{\omega_n} \phi_i(-\omega_n)\, J_{ij}\, \phi_j(\omega_n) \; . \end{aligned} \tag{90}$$

Superohmic damping is qualitatively weaker than ohmic damping and the exponent z_0 is between 1 and 2. For ohmic damping, z_0 is equal to 2. Cases involving no damping (i.e., $z_0 = 1$) and subohmic damping (i.e., $z_0 > 2$), which is qualitatively stronger than the ohmic damping, are discussed at the end of this chapter. The following discusses a single-site constraint for superohmic damping.

The constraint for a single rotor is derived to find the relationship between the damping coefficient and the distance from the critical point. The single site constraint of equation (54) for the superohmic damping is

$$T \sum_{\omega_m} \frac{1}{\epsilon + \gamma \, |\omega_m|^{2/z_0}} = 1 \; . \tag{91}$$

The sum can be transformed into an integral at absolute zero:

$$\int_0^\infty \frac{\mathrm{d}\omega_m}{\epsilon + \gamma \, (\omega_m)^{2/z_0}} = \pi \; . \tag{92}$$

The definition $\epsilon x^{2/z_0} = \gamma(\omega_m)^{2/z_0}$ simplifies this equation to

$$\frac{\epsilon^{\frac{z_0}{2}-1}}{\gamma^{z_0/2}} \int_0^\infty \frac{\mathrm{d}x}{1+x^{2/z_0}} = \pi \ .$$

Because the above integral is a constant c, it yields the relationship between distance from the critical point ϵ and the damping coefficient γ:

$$\epsilon = c(1/\gamma)^{z_0/(2-z_0)} \ . \tag{93}$$

The distance from the critical point in superohmic damping has a power law dependence on the damping coefficient. For ohmic damping, however, the distance from the critical point is exponentially dependent on the damping coefficient (i.e. equation (55)).

5.2. APPLICATION OF THE STRONG-DISORDER RENORMALIZATION GROUP METHOD

The recursion relationships are derived below using technique similar to that outlined above in section 4.3 for ohmic damping. In the Landau-Ginzburg-Wilson functional of equation (90), the largest local energy (i.e., $\Omega = \max(\epsilon_i, J_{ij})$) is first identified. In the first case discussed below, ϵ_2 is the largest local energy in a cluster of sites 1, 2, and 3.

5.2.1. Decimation of a site. Rotor ϕ_2 is eliminated because ϵ_2 is much greater than J_{12} and J_{23}, and the rotor does not contribute to the order parameter. For site 2, the partition function is

$$Z = \int \mathrm{d}\phi_1^*(\omega_n)\,\mathrm{d}\phi_1(\omega_n)\,\mathrm{d}\phi_2(\omega_n)\,\mathrm{d}\phi_2^*(\omega_n)\,\mathrm{d}\phi_3(\omega_n)\,\mathrm{d}\phi_3^*(\omega_n)\,e^{-(S_0+S_1)}$$

with

$$S_0 = T\sum_{\omega_n} (\epsilon_2 + \gamma_2|\omega_n|^{2/z_0})\,|\phi_2(\omega_n)|^2$$

and

$$S_1 = -T\left[\sum_{\omega_n} \phi_1(-\omega_n)\, J_{12}\, \phi_2(\omega_n) + \sum_{\omega_n} \phi_2(-\omega_n)\, J_{23}\, \phi_3(\omega_n)\right] .$$

The expansion in terms of cumulants (i.e., equation (B.1)) yields the effective interaction $\tilde{J}_{13}$ between rotors at sites 1 and 3:

$$\begin{aligned} -T\sum_{\omega_n} \phi_1(-\omega_n)\, \tilde{J}_{13}\phi_3(\omega_n) &= -\ln\left\langle e^{S_1}\right\rangle_0 \\ &= -\left\langle S_1\right\rangle_0 - \frac{1}{2}\left(\left\langle S_1^2\right\rangle_0 - \left\langle S_1\right\rangle_0^2\right) + O(S_1^3) , \end{aligned} \tag{94}$$

and the partition function after elimination of rotor ϕ_2 is

$$\tilde{Z} = \int \mathrm{d}\phi_1^*(\omega_n)\, \mathrm{d}\phi_1(\omega_n)\, \mathrm{d}\phi_3^*(\omega_n)\, \mathrm{d}\phi_3(\omega_n)\, e^{T\sum_{\omega_n} \phi_1(-\omega_n)\, \tilde{J}_{13}\, \phi_3(\omega_n)} .$$

The term $\langle S_1\rangle_0$, which is the average of S_1 with respect to S_0, is given by

$$\begin{aligned} \left\langle S_1\right\rangle_0 = &\frac{-T\sum_{\omega_n} \phi_1(-\omega_n)\, J_{12} \int \mathrm{d}\phi_2(\omega_n)\, \mathrm{d}\phi_2^*(\omega_n)\, \phi_2(\omega_n)\, e^{-S_0}}{\int \mathrm{d}\phi_2(\omega_n)\, \mathrm{d}\phi_2^*(\omega_n)\, e^{-S_0}} \\ &- \frac{T\sum_{\omega_n} \phi_3(\omega_n)\, J_{23} \int \mathrm{d}\phi_2(\omega_n)\, \mathrm{d}\phi_2^*(\omega_n)\phi_2(-\omega_n)\, e^{-S_0}}{\int \mathrm{d}\phi_2(\omega_n)\, \mathrm{d}\phi_2^*(\omega_n)\, e^{-S_0}} . \end{aligned}$$

The integrals vanish due to symmetry. Therefore,

$$\left\langle S_1\right\rangle_0 = 0. \tag{95}$$

The term $\langle S_1^2\rangle_0$ is given by

$$\begin{aligned} \left\langle S_1^2\right\rangle_0 = &\frac{T\sum_{\omega_n} |\phi_1(\omega_n)|^2\, J_{12}^2 \int \mathrm{d}\phi_2(\omega_n)\, \mathrm{d}\phi_2^*(\omega_n)\, |\phi_2(\omega_n)|^2\, e^{-S_0}}{\int \mathrm{d}\phi_2(\omega_n)\, \mathrm{d}\phi_2^*(\omega_n)\, e^{-S_0}} \\ &+ \frac{T\sum_{\omega_n} |\phi_3(\omega_n)|^2\, J_{23}^2 \int \mathrm{d}\phi_2(\omega_n)\, \mathrm{d}\phi_2^*(\omega_n)\, |\phi_2(\omega_n)|^2\, e^{-S_0}}{\int \mathrm{d}\phi_2(\omega_n)\, \mathrm{d}\phi_2^*(\omega_n)\, e^{-S_0}} \\ &+ \frac{2T\sum_{\omega_n} \phi_1(-\omega_n)\, J_{12}J_{23}\, \phi_3(\omega_n) \int \mathrm{d}\phi_2(\omega_n)\, \mathrm{d}\phi_2^*(\omega_n)\, |\phi_2(\omega_n)|^2\, e^{-S_0}}{\int \mathrm{d}\phi_2(\omega_n)\, \mathrm{d}\phi_2^*(\omega_n)\, e^{-S_0}} , \end{aligned}$$

which is solved by using equation (C.3):

$$\langle S_1^2 \rangle_0 = T \sum_{\omega_n} \left[\frac{J_{12}^2 \, |\phi_1(\omega_n)|^2}{\epsilon_2 + \gamma_2 |\omega_n|^{2/z_0}} + \frac{J_{23}^2 \, |\phi_3(\omega_n)|^2}{\epsilon_2 + \gamma_2 |\omega_n|^{2/z_0}} + \frac{2 J_{12} J_{23} \, \phi_1(-\omega_n) \phi_3(\omega_n)}{\epsilon_2 + \gamma_2 |\omega_n|^{2/z_0}} \right] . \quad (96)$$

The first two terms in above equation are subleading corrections to ϵ_1 and ϵ_3 respectively. The last term is the effective interaction between rotors ϕ_1 and ϕ_3. In the low frequency limit, $\gamma_2 |\omega_n|^{2/z_0} / \epsilon_2$ is less than 1. Hence, the denominator in the equation (96) can be simplified as

$$\frac{1}{\epsilon_2 + \gamma_2 |\omega_n|^{2/z_0}} \approx \frac{1}{\epsilon_2} . \quad (97)$$

Thus, equations (94), (95), (96), and (97) yield the effective interaction:

$$\tilde{J}_{13} \approx \frac{J_{12} \, J_{23}}{\epsilon_2} , \quad (98)$$

where higher order cumulants are discarded in the cumulant expansion. This recursion relationship is similar to that obtained for the ohmic damping (which is represented by equation (60)). In both cases, the recursion relationship comes from second-order perturbation theory; thus, it is independent of z_0.

5.2.2. Decimation of a bond. A cluster of sites 2 and 3 is considered for the second case, where the bond J_{23} is the largest local energy. Hence, J_{23} is much greater than ϵ_2 and ϵ_3, and rotors ϕ_2 and ϕ_3 act as a single rotor $\tilde{\phi}_2$. For this cluster, the functional is

$$\begin{aligned} S = T \sum_{\omega_n} & -\phi_2(-\omega_n) \, J_{23} \, \phi_3(\omega_n) + (\epsilon_2 + \gamma_2 |\omega_n|^{2/z_0}) \, |\phi_2(\omega_n)|^2 \\ & + (\epsilon_3 + \gamma_3 |\omega_n|^{2/z_0}) \, |\phi_3(\omega_n)|^2 . \end{aligned} \quad (99)$$

It is simplified in the eigenbasis of ψ_+ and ψ_-. Thus, equation (99) in the matrix form is

$$S = T \sum_{\omega_n} \begin{pmatrix} \phi_2(-\omega_n) & \phi_3(-\omega_n) \end{pmatrix} \begin{pmatrix} \alpha_2 & -\frac{J_{23}}{2} \\ -\frac{J_{32}}{2} & \alpha_3 \end{pmatrix} \begin{pmatrix} \phi_2(\omega_n) \\ \phi_3(\omega_n) \end{pmatrix} ,$$

where α_2 is equal to $\epsilon_2 + \gamma_2|\omega_n|^{2/z_0}$ and α_3 is equal to $\epsilon_3 + \gamma_3|\omega_n|^{2/z_0}$. Eigenvalues of above matrix are

$$\begin{aligned} E_+ =& \frac{(\alpha_2 + \alpha_3) + \sqrt{(\alpha_2 - \alpha_3)^2 + J_{23}^2}}{2} \text{ and} \\ E_- =& \frac{(\alpha_2 + \alpha_3) - \sqrt{(\alpha_2 - \alpha_3)^2 + J_{23}^2}}{2} \end{aligned} \tag{100}$$

with eigenvectors

$$\begin{aligned} \psi_+ =& \cos\left(\frac{\theta}{2}\right)\phi_2(\omega_n) + \sin\left(\frac{\theta}{2}\right)\phi_3(\omega_n) \text{ and} \\ \psi_- =& \sin\left(\frac{\theta}{2}\right)\phi_2(\omega_n) + \cos\left(\frac{\theta}{2}\right)\phi_3(\omega_n) , \end{aligned} \tag{101}$$

where $\tan\theta$ is equal to $J_{23}/(\alpha_3 - \alpha_2)$. Thus, the functional of equation (99) is

$$S' = T\sum_{\omega_n} E_+|\psi_+(\omega_n)|^2 + E_-|\psi_-(\omega_n)|^2 \tag{102}$$

in the eigenbasis.

The energy eigenvalue E_- (of equation (100)) is

$$E_- = \frac{\alpha_2 + \alpha_3 - J_{23}}{2} ,$$

where higher order terms in its expansion are discarded because J_{23} is much greater than ϵ_2 and ϵ_3. Therefore, the damping coefficient is

$$\tilde{\gamma} = \gamma_2 + \gamma_3 ,$$

and the effective distance from the critical point is

$$\tilde{\epsilon} = \epsilon_2 + \epsilon_3 - J_{23} .$$

This distance is approximated as

$$\tilde{\epsilon} \approx X_2 + X_3 ,$$

where X_2 is equal to $\epsilon_2 - \frac{J_{23}}{2}$ and X_3 is equal to $\epsilon_3 - \frac{J_{23}}{2}$. The length constraint at sites 2 and 3 are used to find this effective distance, which is shown below in appendix G. Thus, equation (G.11) yields

$$\tilde{\epsilon}^{-x} \approx \alpha(\epsilon_2^{-x} + \epsilon_3^{-x}) \,, \tag{103}$$

where x is equal to $1 - 2/z_0$, α is a constant, and ϵ_2, ϵ_3 are given by equation (93).

Thus, the general form of recursion relationships for decimation of sites and bonds is

$$\tilde{J}_{i-1,i+1} \approx \frac{J_{i-1,i}\, J_{i,i+1}}{\epsilon_1}$$
$$\tilde{\epsilon}^{-x} \approx \alpha(\epsilon_i^{-x} + \epsilon_{i+1}^{-x}) \,.$$

The renormalization group flows and observable quantities for these recursion relationships in a one-dimensional system are calculated in [68] and the transition found is of Kosterlitz-Thouless[35] type. The main difference between superohmic and ohmic damping is reflected in the dynamical scaling form, which is conventional power-law type in the former and activated in the latter.

For the no-damping case (i.e., when z_0 is equal to 1), dynamic scaling is of the power-law type, and equation (103) is reduced to

$$\frac{1}{\tilde{\epsilon}} \approx \alpha(\frac{1}{\epsilon_2} + \frac{1}{\epsilon_3}) \,,$$

which is the result derived in [69] for a one-dimensional system of bosons with strong disorder. The corresponding flow equations are given in [69], and the transition is again of Kosterlitz-Thouless type.

For the subohmic case (i.e., when z_0 is grater than 2), the integral in equation (92) is reduced to

$$\gamma_c = \pi(1 - 2/z_0)\Lambda^{2/z_0 - 1}$$

in the limit ϵ tending to 0. The integral in equation (92) has no solution if the damping

[35]For the details of Kosterlitz-Thouless transition see, e.g., [14, 4].

coefficient γ is greater than γ_c. Thus, a cluster freezes for a damping coefficient greater than γ_c. The damping coefficients are summed under the recursion relationships. Thus, the dynamics of the transition eventually freezes and the transition is destroyed by smearing [70].

6. SUMMARY AND CONCLUSIONS

In summary, quantum phase transitions with disorder were studied in the presence of ohmic damping. The Landau-Ginzburg-Wilson functional for these quantum phase transitions was derived using the standard techniques of [57, 58, 59]. The resulting functional was then modified by expressing it in discrete space and by making the number of order-parameter components N large. The first modification allows the application of the strong-disorder renormalization group method to the functional. This method is a real space method and therefore, expressing the functional in discrete space is necessary. The second modification turns the functional into a self-consistent Gaussian problem that can be solved analytically. The strong-disorder renormalization group method was applied to this modified functional to find the recursion relationships for the coupling constants. From these relationships, the renormalization group flow equations were derived [41] and the critical behavior was studied. The observable quantities at and near the critical point were discussed. Although these calculations were performed within the limit of a large number of order-parameter components (i.e. for a large N), they were shown to be valid for all N greater than 1. A generalization of this problem, that is quantum phase transitions in the presence of superohmic damping, was also studied. The recursion relationships for this case were again derived by applying the strong-disorder renormalization group method. The critical behavior for these recursion relationships is obtained in [68]. The following discusses the limitations of this theory and provides a perspective of the results.

The theory is developed on the basis of the so-called Hertz-Millis approach to quantum phase transitions. The assumption, which is suitable for transition metal compounds, in this approach is that the quasi-particles do not break up at the transition. For heavy-fermion systems, the theory relies on the assumption that the Kondo effect survives at low temperatures. Several experimental systems listed in [42, 43] are in contradiction with this assumption. Thus, the Landau-Ginzburg-Wilson functional is inappropriate for these systems. Apart from this difficulty, the Landau-Ginzburg-Wilson functional does not take into account other complications such as long-range interactions between order-parameter fluctuations. These complications are present

in real systems and can affect the characteristics of a phase transition at absolute zero and at a very low temperature. Nevertheless, the results obtained here provide insight in a disorder-dominated quantum phase transition with ohmic damping.

The investigation shows that quantum phase transitions in the presence of ohmic dissipation are strongly influenced by disorder. The critical point is an infinite-randomness critical point, which is in the universality class same as that of random transverse-field Ising model [40, 41]. This result is in agreement with the numerical study carried out in [71] for a one-dimensional Landau-Ginzburg-Wilson functional for a large N. At the critical point, the observable quantities (i.e., specific heat and susceptibility) follow activated scaling (i.e., power-law dependence of logarithmic variables) rather than conventional power-law dependence. The behavior of observable quantities is of power-law type in the quantum Griffiths paramagnetic region. From the general classification of rare regions in [22, 67], the dimension of rare regions in a quantum phase transition with ohmic dissipation is equal to the lower critical dimension of the system. The behavior of observable quantities at the critical point and in the Griffiths region are in agreement with this classification.

The shape of the phase boundary near the critical point is derived from the scaling form of susceptibility. The critical temperature predicted in this region is proportional to $e^{-r^{-\nu\psi}}$, where r is the distance from the critical point. Critical temperatures and the resulting shape of the phase boundary near the apparent critical point in $CePd_{1-x}Rh_x$ (i.e., figure (4.1)) are in agreement with this prediction. The susceptibility in the Griffiths paramagnetic phase is proportional to $T^{d/z-1}$ at a specific impurity concentration (i.e. at a constant r). The susceptibility measurements for $CePd_{1-x}Rh_x$ (i.e., figure (4.2)) and $Ni_{1-x}V_x$ (i.e., figure (4.4)) at various impurity concentrations display this power-law temperature dependence in the Griffiths paramagnetic region. The susceptibility measurements for $Ni_{1-x}V_x$ are in agreement with the theoretical prediction in the range of 10 to 300 K. The superconductor-metal phase transition in extremely thin nanowires [47, 48] occurring as a function of thickness of wire can also be explained by this theory. This transition is studied in the absence of disorder in references [72, 73] using one dimensional Landau-Ginzburg-Wilson functional with ohmic dissipation. The magnetic impurities that are distributed randomly

on the surface of nanowires introduce disorder in the system. Hence, the thermodynamics of this transition can be described by this theory.

A brief discussion of other dissipation scenarios is as follows: The recursion relationships derived for superohmic damping are similar except for the one derived for the effective distance from the critical point. The resulting phase transition for these recursion relationships is of Kosterlitz-Thouless type [68] and has conventional power-law scaling. The transition for the subohmic damping case is destroyed by smearing. In the absence of dissipation, the recursion relationships are similar to a system of bosons with strong disorder. The transition for this case is of Kosterlitz-Thouless type.

The investigation so far has focused on the critical point and the disordered region of a phase diagram. Beyond this theory, there is much complex physics yet to be explored in these regions. The physics in the ordered phase of the phase diagram also poses challenges. It seems that a comprehensive theory of quantum phase transitions has a long way to go.

APPENDIX A

HUBBARD INTERACTION IN TERMS OF SPIN DENSITY

The Hubbard interaction can be represented in terms of the spin-density vector in discrete space, which is shown in the following. This result can be mapped to continuum space.

In discrete space, the spin-density vector at a site is defined as

$$\begin{aligned}\mathbf{n}_s &= \sum_{i,j} C_i^\dagger \hat{\sigma}_{ij} C_j \\ &= \frac{1}{2}\left[\hat{x}(C_\uparrow^\dagger C_\downarrow + C_\downarrow^\dagger C_\uparrow) + \hat{y}(-iC_\uparrow^\dagger C_\downarrow + iC_\downarrow^\dagger C_\uparrow) + \hat{z}(C_\uparrow^\dagger C_\uparrow - C_\downarrow^\dagger C_\downarrow)\right] .\end{aligned}$$

The dot product of the spin-density vector is

$$\mathbf{n}_s \cdot \mathbf{n}_s = \frac{n_\uparrow^2 + n_\downarrow^2}{4} + \frac{(n_\uparrow + n_\downarrow)}{2} - \frac{3n_\uparrow n_\downarrow}{2} .$$

Since $n_\uparrow$ is a product of creation and annihilation operators of a fermion, $n_\uparrow^2$ is equal to 1 or 0. Thus, $n_\uparrow^2$ is equal to $n_\uparrow$; likewise, $n_\downarrow^2$ is equal to $n_\downarrow$. These results transform the above equation into

$$n_\uparrow n_\downarrow = \frac{n_\uparrow + n_\downarrow}{2} - \frac{2}{3}\mathbf{n}_s \cdot \mathbf{n}_s .$$

For a lattice with l sites, the Hubbard interaction can thus be replaced as

$$u\sum_l n_{l\uparrow} n_{l\downarrow} = -\frac{2u}{3}\sum_l \mathbf{n}_{l\,s} \cdot \mathbf{n}_{l\,s} , \tag{A.1}$$

where the term $(n_\uparrow + n_\downarrow)$ is absorbed in chemical potential as a shift.

APPENDIX B

EXPANSION IN TERMS OF CUMULANTS

The expansion of $\ln \langle e^x \rangle_{x_0}$ in terms of cumulants is

$$\begin{aligned}\ln \langle e^x \rangle_{x_0} =& \langle x \rangle_{x_0} + \langle x^2 \rangle_{x_0} - \langle x \rangle_{x_0}^2 + \langle x^3 \rangle_{x_0} - 3\langle x^2 \rangle_{x_0} \langle x \rangle_{x_0} + 2\langle x \rangle_{x_0}^3 \\ &+ \langle x^4 \rangle_{x_0} - 3\langle x^2 \rangle_{x_0}^2 + 4\langle x \rangle_{x_0} \langle x^3 \rangle_{x_0} - 6\langle x \rangle_{x_0}^4 + \dots . \end{aligned} \tag{B.1}$$

APPENDIX C

INTEGRATION OVER A COMPLEX VARIABLE

The following solves the integral

$$\frac{\int |\phi|^2 \exp(-a|\phi|^2)\, \mathrm{d}\phi\, \mathrm{d}\phi^*}{\int \exp(-a|\phi|^2)\, \mathrm{d}\phi\, \mathrm{d}\phi^*} \,.$$

If 'Reϕ' and 'Imϕ' are real and imaginary parts of a rotor variable ϕ, then the integral in the numerator yields

$$2i \int \left(\mathrm{Re}^2\phi + \mathrm{Im}^2\phi\right) \exp\left[-a\left(\mathrm{Re}^2\phi + \mathrm{Im}^2\phi\right)\right]\, \mathrm{d}\left(\mathrm{Re}\phi\right)\, \mathrm{d}\left(\mathrm{Im}\phi\right) \,,$$

where $\mathrm{d}\phi\, \mathrm{d}\phi^*$ is equal to $2i\, \mathrm{d}\left(\mathrm{Re}\phi\right)\, \mathrm{d}\left(\mathrm{Im}\phi\right)$. Real and imaginary parts are separated to solve the integral. Thus,

$$\begin{aligned} &2i \int \left(\mathrm{Re}^2\phi\right) \exp\left[-a\left(\mathrm{Re}^2\phi\right)\right]\, \mathrm{d}\left(\mathrm{Re}\phi\right) \int \exp\left[-a\left(\mathrm{Im}^2\phi\right)\right]\, \mathrm{d}\left(\mathrm{Im}\phi\right) \\ &\quad + 2i \int \left(\mathrm{Im}^2\phi\right) \exp\left[-a\left(\mathrm{Im}^2\phi\right)\right]\, \mathrm{d}\left(\mathrm{Im}\phi\right) \int \exp\left[-a\left(\mathrm{Re}^2\phi\right)\right]\, \mathrm{d}\left(\mathrm{Re}\phi\right) \,. \end{aligned}$$

The solution of Gaussian integrals yields the numerator:

$$\int |\phi|^2 \exp\left(-a|\phi|^2\right)\, \mathrm{d}\phi\, \mathrm{d}\phi^* = \frac{i\pi}{2a^2} \,. \tag{C.1}$$

Using the same technique, the integral in the denominator is calculated as

$$\int \exp(-a|\phi|^2)\, \mathrm{d}\phi\, \mathrm{d}\phi^* = \frac{i\pi}{2a} \,. \tag{C.2}$$

Thus, equations (C.1) and (C.2) yield

$$\frac{\int |\phi|^2 \exp\left(-a|\phi|^2\right)\, \mathrm{d}\phi\, \mathrm{d}\phi^*}{\int \exp\left(-a|\phi|^2\right)\, \mathrm{d}\phi\, \mathrm{d}\phi^*} = \frac{1}{a} \,. \tag{C.3}$$

APPENDIX D

EVALUATION OF AN INTEGRAL WITH A FERMI-STEP FUNCTION

The integral

$$\int d\mathbf{q}_1 \frac{\Theta\left(\mu - \frac{\mathbf{q}_1^2}{2}\right)}{\mathbf{q}_1 \cdot \mathbf{q} + \frac{\mathbf{q}^2}{2} + i\omega_n} \tag{D.1}$$

is evaluated here. The definition $\rho = \frac{\mathbf{q}^2}{2} + i\omega_n$ reduces the above integral to

$$\int_0^{K_F} \int_0^{\pi} \int_0^{2\pi} \frac{\mathrm{q}_1^2 \sin\theta \, \mathrm{dq}_1 \, \mathrm{d}\theta \, \mathrm{d}\phi}{\mathrm{q}_1 \mathrm{q} \cos\theta + \rho} \, .$$

Therefore, the solution yields

$$\begin{aligned} &\int d\mathbf{q}_1 \frac{\Theta\left(\mu - \frac{\mathbf{q}_1^2}{2}\right)}{\mathbf{q}_1 \cdot \mathbf{q} + \frac{\mathbf{q}^2}{2} + i\omega_n} \\ &= \frac{2\pi}{\mathrm{q}} \left[\left(\frac{K_F^2}{2} - \frac{\rho^2}{2\mathrm{q}^2} \right) [\ln(-\mathrm{q}K_F + \rho) - \ln(\mathrm{q}K_F + \rho)] - \frac{\rho K_F}{\mathrm{q}} \right] . \end{aligned} \tag{D.2}$$

APPENDIX E

DERIVATION OF DYNAMIC SUSCEPTIBILITY

The respective Fourier transforms of the creation and annihilation Grassman fields are

$$\psi_i(\mathbf{x},\tau) = T\sum_{\omega_n}\int \mathrm{d}\mathbf{q}\,\psi_i(\mathbf{q},\omega_n)\,e^{i(\mathbf{q}\cdot\mathbf{x}-\omega_n\tau)} \text{ and}$$
$$\bar{\psi}_i(\mathbf{x},\tau) = T\sum_{\omega_n}\int \mathrm{d}\mathbf{q}\,\bar{\psi}_i(\mathbf{q},\omega_n)\,e^{-i(\mathbf{q}\cdot\mathbf{x}-\omega_n\tau)}\ .$$

Use of these to obtain S_0 (i.e., equation (40)) in Fourier space yields

$$S_0(\mathbf{q},\omega_n) = T\sum_{\omega_n}\int \mathrm{d}\mathbf{q}\sum_i\left[\bar{\psi}_i(\mathbf{q},\omega_n)\left(-\frac{\mathbf{q}^2}{2}+\mu-i\omega_n\right)\psi_i(\mathbf{q},\omega_n)\right]. \qquad \text{(E.1)}$$

Similarly, the product of spin-density vectors in Fourier space is

$$\begin{aligned}\mathbf{n}_s(\mathbf{x},\tau)\cdot\mathbf{n}_s(\mathbf{x}',\tau') =& T^4\sum_{\omega_{n_1}\,\omega_{n_2}\,\omega_{n_3}\,\omega_{n_4}}\int \mathrm{d}\mathbf{q}_1\,\mathrm{d}\mathbf{q}_2\,\mathrm{d}\mathbf{q}_3\,\mathrm{d}\mathbf{q}_4\,e^{i[(\mathbf{q}_2-\mathbf{q}_1)\cdot\mathbf{x}-(\omega_{n_2}-\omega_{n_1})\tau]}\\ &\times e^{-i[(\mathbf{q}_3-\mathbf{q}_4)\cdot\mathbf{x}'-(\omega_{n_3}-\omega_{n_4})\tau']}\\ &\times\sum_{ijj'i'}\bar{\psi}_i(\mathbf{q}_1,\omega_{n_1})\frac{\hat{\sigma}_{ij}}{2}\psi_j(\mathbf{q}_2,\omega_{n_2})\cdot\bar{\psi}_{i'}(\mathbf{q}_3,\omega_{n_3})\frac{\hat{\sigma}_{i'j'}}{2}\psi_{j'}(\mathbf{q}_4,\omega_{n_4})\ .\end{aligned} \qquad \text{(E.2)}$$

Therefore, equations (E.1) and (E.2) yield the thermal average of spin-density vectors:

$$\langle\mathbf{n}_s(\mathbf{x},\tau)\cdot\mathbf{n}_s(\mathbf{x}'\tau')\rangle_{S_0} = \frac{\prod_i\int \mathrm{D}\psi_i\,\mathrm{D}\bar{\psi}_i\,\mathbf{n}_s(\mathbf{x},\tau)\cdot\mathbf{n}_s(\mathbf{x}',\tau')\,e^{-S_0(\mathbf{q},\omega_n)}}{\prod_i\int \mathrm{D}\psi_i\,\mathrm{D}\bar{\psi}_i\,e^{-S_0(\mathbf{q},\omega_n)}}\ .$$

Application of the Wick theorem[36] contracts the Grassman fields $\bar{\psi}_i(\mathbf{q}_1,\omega_{n_1})\,\psi_{j'}(\mathbf{q}_4,\omega_{n_4})$ and $\psi_j(\mathbf{q}_2,\omega_{n_2})\,\bar{\psi}_{i'}(\mathbf{q}_3,\omega_{n_3})$. This contraction implies

$$\mathbf{q}_1=\mathbf{q}_4 \quad ; \quad \mathbf{q}_2=\mathbf{q}_3$$
$$\omega_{n_1}=\omega_{n_4} \quad ; \quad \omega_{n_2}=\omega_{n_3}\ .$$

[36] See, e.g., [54], [60].

Hence,

$$\langle \mathbf{n}_s(\mathbf{x},\tau)\cdot\mathbf{n}_s(\mathbf{x}'\tau')\rangle_{S_0} = \alpha T^2 \sum_{\omega_{n_1}\omega_{n_2}} \int \mathrm{d}\mathbf{q}_1\,\mathrm{d}\mathbf{q}_2 \frac{e^{i[(\mathbf{q}_2-\mathbf{q}_1)(\mathbf{x}-\mathbf{x}')-(\omega_{n_2}-\omega_{n_1})(\tau-\tau')]}}{\left(-\frac{\mathbf{q}_1^2}{2}+\mu-i\omega_{n_1}\right)\left(-\frac{\mathbf{q}_2^2}{2}+\mu-i\omega_{n_2}\right)},$$

where α is equal to $\sum_{ij}\hat{\sigma}_{ij}\cdot\hat{\sigma}_{ji}$. Therefore, the dynamic susceptibility $\chi(\mathbf{q},\omega_n)$ (i.e., equation (45)) is given by

$$\begin{aligned}\chi(\mathbf{q},\omega_n) &= \alpha \int \mathrm{d}\mathbf{x}'' \int_0^\beta \mathrm{d}\tau'' T^2 \sum_{\omega_{n_1}\omega_{n_2}} \int \mathrm{d}\mathbf{q}_1\,\mathrm{d}\mathbf{q}_2\, e^{i[(\mathbf{q}_2-\mathbf{q}_1-\mathbf{q})\cdot\mathbf{x}''-(\omega_{n_2}-\omega_{n_1}-\omega_n)\tau'']} \\ &\quad\times \frac{1}{\left(-\frac{\mathbf{q}_1^2}{2}+\mu-i\omega_{n_1}\right)\left(-\frac{\mathbf{q}_2^2}{2}+\mu-i\omega_{n_2}\right)} \\ &= \alpha T \sum_{\omega_{n_1}} \int \mathrm{d}\mathbf{q}_1 \frac{1}{\left(-\frac{\mathbf{q}_1^2}{2}+\mu-i\omega_{n_1}\right)\left(-\frac{(\mathbf{q}_1+\mathbf{q})^2}{2}+\mu-i(\omega_{n_1}+\omega_n)\right)}.\end{aligned}$$

The sum over ω_{n_1} can be transformed into an integral:

$$\chi(\mathbf{q},\omega_n) = \alpha \int \mathrm{d}\mathbf{q}_1 \int \mathrm{d}\omega_{n_1} \frac{1}{\left(-\frac{\mathbf{q}_1^2}{2}+\mu-i\omega_{n_1}\right)\left(-\frac{(\mathbf{q}_1+\mathbf{q})^2}{2}+\mu-i(\omega_{n_1}+\omega_n)\right)}.$$

The integral over ω_{n_1} is simplified by defining z as $-i(\omega_{n_1}+\omega_n)$. Thus,

$$\chi(\mathbf{q},\omega_n) = \alpha \int \mathrm{d}\mathbf{q}_1 \int \frac{i\,\mathrm{d}z}{(z+i\omega_n-\zeta)(z-\zeta')},$$

where ζ is equal to $\frac{\mathbf{q}_1^2}{2}-\mu$ and ζ' is equal to $\frac{(\mathbf{q}_1+\mathbf{q})^2}{2}-\mu$. The residue theorem gives the following solution:

$$\chi(\mathbf{q},\omega_n) = 2\pi\alpha \int \mathrm{d}\mathbf{q}_1 \left[\frac{\Theta(-\zeta')}{\zeta'-\zeta+i\omega_n} - \frac{\Theta(-\zeta)}{\zeta'-\zeta+i\omega_n}\right],$$

where Θ is the Fermi step function. Substitution of ζ and ζ' in above equation yields

$$\chi(\mathbf{q},\omega_n) = 2\pi\alpha \left[\int \mathrm{d}\mathbf{q}' \frac{\Theta\left(\mu-\frac{\mathbf{q}'^2}{2}\right)}{\mathbf{q}'\cdot\mathbf{q}-\frac{\mathbf{q}^2}{2}+i\omega_n} - \int \mathrm{d}\mathbf{q}_1 \frac{\Theta\left(\mu-\frac{\mathbf{q}_1^2}{2}\right)}{\mathbf{q}_1\cdot\mathbf{q}+\frac{\mathbf{q}^2}{2}+i\omega_n}\right],$$

where $\mathbf{q}'$ is equal to $\mathbf{q}_1+\mathbf{q}$. The definitions $\rho' = -\frac{\mathbf{q}^2}{2}+i\omega_n$ and $\rho = \frac{\mathbf{q}^2}{2}+i\omega_n$

reduce both integrals in the above equation to equation (D.1). Thus, the solution (i.e., equation (D.2)) of these integrals gives

$$\chi(\mathbf{q},\omega_n) = \frac{4\pi^2\alpha}{\mathrm{q}}\left[\left(\frac{K_F^2}{2}-\frac{\rho^2}{2\mathrm{q}^2}\right)\left[\ln(-\mathrm{q}K_F+\rho)-\ln(\mathrm{q}K_F+\rho)\right]\right.$$
$$\left.+\left(\frac{K_F^2}{2}-\frac{\rho'^2}{2\mathrm{q}^2}\right)\left[\ln(-\mathrm{q}K_F+\rho')-\ln(\mathrm{q}K_F+\rho')\right]+\frac{(\rho'-\rho)K_F}{\mathrm{q}}\right]. \tag{E.3}$$

Within the limit $\mathrm{q}/K_F << 1$ and $\omega_n/\mathrm{q}K_F << 1$, which is the relevant limit for the ferromagnetic quantum phase transition, the above logarithmic terms can be simplified as

$$\ln(-\mathrm{q}K_F+\rho) = \ln\left(-1-\frac{\mathrm{q}}{2K_F}+i\frac{\omega_n}{\mathrm{q}K_F}\right)+\ln(\mathrm{q}K_F) = i\pi\mathrm{sgn}(\omega_n)+\ln(\mathrm{q}K_F),$$
$$\ln(\mathrm{q}K_F+\rho) = \left(-\frac{\mathrm{q}}{2K_F}+i\frac{\omega_n}{\mathrm{q}K_F}\right)+\ln(\mathrm{q}K_F),$$
$$\ln(-\mathrm{q}K_F+\rho') = \ln\left(-1+\frac{\mathrm{q}}{2K_F}+i\frac{\omega_n}{\mathrm{q}K_F}\right)+\ln(\mathrm{q}K_F) = i\pi\mathrm{sgn}(\omega_n)+\ln(\mathrm{q}K_F),$$
$$\text{and } \ln(\mathrm{q}K_F+\rho') = \left(\frac{\mathrm{q}}{2K_F}+i\frac{\omega_n}{\mathrm{q}K_F}\right)+\ln(\mathrm{q}K_F),$$

where sgn is a sign function. Since $\rho' = \rho+\mathrm{q}^2$, the dynamic susceptibility reduces to

$$\chi(\mathbf{q},\omega_n) = \frac{4\pi^2\alpha}{\mathrm{q}}\left[\left(\frac{K_F^2}{2}-\frac{\rho^2}{2\mathrm{q}^2}\right)\frac{\mathrm{q}}{K_F}\right.$$
$$\left.+\left(\frac{\mathrm{q}^2}{2}+\rho\right)\left(i\pi\mathrm{sgn}(\omega_n)-i\frac{\omega_n}{\mathrm{q}K_F}-\frac{\mathrm{q}}{2K_F}\right)+\mathrm{q}K_F\right].$$

Substitution of ρ and of the result $\omega_n\mathrm{sgn}(\omega_n) = |\omega_n|$ in the above equation yields

$$\chi(\mathbf{q},\omega_n) = 4\pi^2\alpha\left(\frac{3K_F}{2}-\frac{\mathbf{q}^2}{8K_F}-\frac{\pi|\omega_n|}{\mathrm{q}}+\frac{3\omega_n^2}{\mathbf{q}^2K_F}\right).$$

Since the last term in the above equation is a subleading term, the dynamic susceptibility is

$$\chi(\mathbf{q},\omega_n) = 4\pi^2\alpha\left(\frac{3K_F}{2} - \frac{\mathbf{q}^2}{8K_F} - \frac{\pi|\omega_n|}{\mathrm{q}}\right) . \tag{E.4}$$

APPENDIX F

DISTANCE FROM THE CRITICAL POINT OF A TWO-SITE CLUSTER FOR OHMIC DAMPING

The distance from the critical point of a cluster formed by combining rotors ϕ_2 and ϕ_3 is given by equation (65) as

$$\tilde{\epsilon} \approx \frac{\epsilon_2\epsilon_3 - J_{23}^2/4}{J_{23}} .$$

The length constraints at sites 2 and 3 for a particular frequency simplify this expression. The following calculates this constraint at site 2 by using the thermal average of $\phi_2(\omega_m)$, which is

$$\left\langle |\phi_2(\omega_m)|^2 \right\rangle = \frac{\int |\phi_2(\omega_m)|^2 \, \mathrm{d}\phi_2(\omega_n) \, \mathrm{d}\phi_2^*(\omega_n) \, \mathrm{d}\phi_3(\omega_n) \, \mathrm{d}\phi_3^*(\omega_n) \, e^{-S}}{\int \mathrm{d}\phi_2(\omega_n) \, \mathrm{d}\phi_2^*(\omega_n) \, \mathrm{d}\phi_3(\omega_n) \, \mathrm{d}\phi_3^*(\omega_n) \, e^{-S}},$$

where S is defined in equation (61). This average is expressed in the eigenbasis ψ_+ and ψ_- using equation (63):

$$\frac{\int \mathrm{D}[\psi_+\psi_-](\omega_n) \, (\cos^2(\theta/2)|\psi_+(\omega_m)|^2 + \sin^2(\theta/2)|\psi_-(\omega_m)|^2) \, e^{-S'}}{\int \mathrm{D}[\psi_+\psi_-](\omega_n) \, e^{-S'}} ,$$

where $\mathrm{D}[\psi_+\psi_-](\omega_n)$ is equal to $\mathrm{d}\psi_+(\omega_n) \, \mathrm{d}\psi_+^*(\omega_n) \, \mathrm{d}\psi_-(\omega_n) \, \mathrm{d}\psi_-^*(\omega_n)$ and S' is defined in equation (64). For a frequency ω_m, integrals in the numerator and the denominator split as

$$\frac{\int \mathrm{D}[\psi_+\psi_-](\omega_m)[\cos^2(\theta/2)|\psi_+(\omega_m)|^2 + \sin^2(\theta/2)|\psi_-(\omega_m)|^2] \, e^{-S_{\omega_m}}}{\int \mathrm{D}[\psi_+\psi_-](\omega_m) \, e^{-S_{\omega_m}}}$$
$$\times \frac{\int \mathrm{D}[\psi_+\psi_-](\omega_{n\neq m}) \, e^{-S'}}{\int \mathrm{D}[\psi_+\psi_-](\omega_{n\neq m}) \, e^{-S'}} ,$$

where S_{ω_m} is equal to $T(E_+|\psi_+(\omega_m)|^2 + E_-|\psi_-(\omega_m)|^2)$. The first term above can be

simplified as

$$\cos^2(\theta/2)\left[\frac{\int \mathrm{d}\psi_+(\omega_m)\,\mathrm{d}\psi_+^*(\omega_m)|\psi_+(\omega_m)|^2\,e^{-T\,E_+|\psi_+(\omega_m)|^2}}{\int \mathrm{d}\psi_+(\omega_m)\,\mathrm{d}\psi_+^*(\omega_m)\,e^{-T\,E_+|\psi_+(\omega_m)|^2}}\right.$$
$$\left.\times\frac{\int \mathrm{d}\psi_-(\omega_m)\,\mathrm{d}\psi_-^*(\omega_m)\,e^{-T\,E_-|\psi_-(\omega_m)|^2}}{\int \mathrm{d}\psi_-(\omega_m)\,\mathrm{d}\psi_-^*(\omega_m)\,e^{-T\,E_-|\psi_-(\omega_m)|^2}}\right]$$
$$+\sin^2(\theta/2)\left[\frac{\int \mathrm{d}\psi_-(\omega_m)\,\mathrm{d}\psi_-^*(\omega_m)|\psi_-(\omega_m)|^2\,e^{-T\,E_-|\psi_-(\omega_m)|^2}}{\int \mathrm{d}\psi_-(\omega_m)\,\mathrm{d}\psi_-^*(\omega_m)\,e^{-T\,E_-|\psi_-(\omega_m)|^2}}\right.$$
$$\left.\times\frac{\int \mathrm{d}\psi_+(\omega_m)\,\mathrm{d}\psi_+^*(\omega_m)\,e^{-T\,E_+|\psi_+(\omega_m)|^2}}{\int \mathrm{d}\psi_+(\omega_m)\,\mathrm{d}\psi_+^*(\omega_m)\,e^{-T\,E_+|\psi_+(\omega_m)|^2}}\right]\,.$$

Use of equation (C.3) to solve above integrals yields the thermal average:

$$\begin{aligned}\left\langle|\phi_2(\omega_m)|^2\right\rangle &= \frac{1}{T}\left[\frac{\cos^2(\theta/2)}{E_+}+\frac{\sin^2(\theta/2)}{E_-}\right]\\ &= \frac{4}{T(4\alpha_2\alpha_3-J_{23}^2)}\left[\frac{(\alpha_2+\alpha_3)}{2}+\frac{\cos\theta}{2}\sqrt{(\alpha_2-\alpha_3)^2+J_{23}^2}\right]\,,\end{aligned}$$

where α_2 is equal to $\epsilon_2+\gamma_2|\omega_n|$ and α_3 is equal to $\epsilon_3+\gamma_3|\omega_n|$. However, because

$$\cos\theta = \frac{\alpha_3-\alpha_2}{\sqrt{(\alpha_2-\alpha_3)^2+J_{23}^2}}\,, \tag{F.1}$$

the average is reduced to

$$\left\langle|\phi_2(\omega_m)|^2\right\rangle = \frac{4\alpha_3}{T(4\alpha_2\alpha_3-J_{23}^2)}\,. \tag{F.2}$$

Thus, the constraint (i.e., equation (52)) at site $\phi_2(\omega_m)$ is

$$T\sum_{\omega_m}\frac{4\alpha_3}{(4\alpha_2\alpha_3-J_{23}^2)}=1\,.$$

At zero temperature, the summation becomes an integral:

$$\int_0^\infty \frac{(\epsilon_3+\gamma_3\omega)\,\mathrm{d}\omega}{(\epsilon_2+\gamma_2\omega)(\epsilon_3+\gamma_3\omega)-\frac{J_{23}^2}{4}}=\pi\,. \tag{F.3}$$

The integral is solved by defining

$$\frac{(\epsilon_3+\gamma_3\omega)/\gamma_2\gamma_3}{\omega^2+(\epsilon_2\gamma_3+\gamma_2\epsilon_3)\omega/\gamma_2\gamma_3+(4\epsilon_2\epsilon_3-J_{23}^2)/4\gamma_2\gamma_3}=\frac{A}{B+\omega}+\frac{C}{D+\omega}\,.$$

Thus,

$$\begin{aligned} A+C&=\frac{1}{\gamma_2} \quad , \quad AD+BC=\frac{\epsilon_3}{\gamma_2\gamma_3}, \\ BD&=\frac{4\epsilon_2\epsilon_3-J_{23}^2}{4\gamma_2\gamma_3} \quad , \quad B+D=\frac{\epsilon_2}{\gamma_2}+\frac{\epsilon_3}{\gamma_3}\,. \end{aligned} \tag{F.4}$$

These equations yield B, D, A , and C:

$$\begin{aligned} B&=\frac{1}{2}\left[\left(\frac{\epsilon_2}{\gamma_2}+\frac{\epsilon_3}{\gamma_3}\right)+\sqrt{\left(\frac{\epsilon_2}{\gamma_2}-\frac{\epsilon_3}{\gamma_3}\right)^2+\frac{J_{23}^2}{\gamma_2\gamma_3}}\right] \quad , \quad D=\frac{4\epsilon_2\epsilon_3-J_{23}^2}{4\gamma_2\gamma_3 B} \\ A&=\frac{B\gamma_3-\epsilon_3}{\gamma_2\gamma_3(B-D)} \quad , \quad C=\frac{\epsilon_3-\gamma_3 D}{\gamma_2\gamma_3(B-D)}\,. \end{aligned} \tag{F.5}$$

Hence, the integral (F.3) is

$$\int_0^\Lambda \frac{A}{B+\omega}\,\mathrm{d}\omega+\int_0^\Lambda \frac{C}{D+\omega}\mathrm{d}\omega=\pi\,,$$

where Λ is a high-frequency cut-off. The solution of the above equation is

$$A\ln\left(\frac{B+\Lambda}{B}\right)+C\ln\left(\frac{D+\Lambda}{D}\right)=\pi\,.$$

Because Λ is much greater than B and D, these fractions are defined as $\frac{B+\Lambda}{B}\approx\frac{\Lambda}{B}$ and $\frac{D+\Lambda}{D}\approx\frac{\Lambda}{D}$. Use of the definition of $A+C$ (in equation (F.4)) modifies this equation to

$$A\gamma_2\ln\left(\frac{D}{B}\right)+\ln\left(\frac{\Lambda}{D}\right)=\pi\gamma_2\,. \tag{F.6}$$

Thus, the equation is derived from the constraint at site 2. It is used below with the constraint at site 3 to derive the distance from the critical point. The constraint at site 3 is derived in the following using similar steps. Hence, the thermal average of

$\phi_3(\omega_m)$ is

$$\langle|\phi_3(\omega_m)|^2\rangle = \frac{\int |\phi_3(\omega_m)|^2\, \mathrm{d}\phi_2(\omega_n)\, \mathrm{d}\phi_2^*(\omega_n)\, \mathrm{d}\phi_3(\omega_n)\, \mathrm{d}\phi_3^*(\omega_n)\, e^{-S}}{\int \mathrm{d}\phi_2(\omega_n)\, \mathrm{d}\phi_2^*(\omega_n)\, \mathrm{d}\phi_3(\omega_n)\, \mathrm{d}\phi_3^*(\omega_n)\, e^{-S}},$$

where S is defined in equation (61). The thermal average in the eigenbasis ψ_+ and ψ_- is

$$\frac{\int \mathrm{D}[\psi_+\psi_-](\omega_m)\, (\sin^2(\theta/2)|\psi_+(\omega_m)|^2 + \cos^2(\theta/2)|\psi_-(\omega_m)|^2)\, e^{-S'}}{\int \mathrm{D}[\psi_+\psi_-](\omega_m)\, e^{-S'}}.$$

Integrals in the numerator and the denominator split for a frequency as

$$\frac{\int \mathrm{D}[\psi_+\psi_-](\omega_m)\, (\sin^2(\theta/2)|\psi_+(\omega_m)|^2 + \cos^2(\theta/2)|\psi_-(\omega_m)|^2)\, e^{-S_{\omega_m}}}{\int \mathrm{D}[\psi_+\psi_-](\omega_m)\, e^{-S_{\omega_m}}} \times \frac{\int \mathrm{D}[\psi_+\psi_-](\omega_{n\neq m})\, e^{-S'}}{\int \mathrm{D}[\psi_+\psi_-](\omega_{n\neq m})\, e^{-S'}}.$$

This equation can be further simplified as

$$\begin{aligned}
&\sin^2(\theta/2)\left[\frac{\int \mathrm{d}\psi_+(\omega_m)\, \mathrm{d}\psi_+^*(\omega_m)|\psi_+(\omega_m)|^2\, e^{-T\,E_+|\psi_+(\omega_m)|^2}}{\int \mathrm{d}\psi_+(\omega_m)\, \mathrm{d}\psi_+^*(\omega_m)\, e^{-T\,E_+|\psi_+(\omega_m)|^2}}\right. \\
&\qquad\left. \times \frac{\int \mathrm{d}\psi_-(\omega_m)\, \mathrm{d}\psi_-^*(\omega_m)\, e^{-T\,E_-|\psi_-(\omega_m)|^2}}{\int \mathrm{d}\psi_-(\omega_m)\, \mathrm{d}\psi_-^*(\omega_m)\, e^{-T\,E_-|\psi_-(\omega_m)|^2}}\right] \\
&+\cos^2(\theta/2)\left[\frac{\int \mathrm{d}\psi_-(\omega_m)\, \mathrm{d}\psi_-^*(\omega_m)|\psi_-(\omega_m)|^2\, e^{-T\,E_-|\psi_-(\omega_m)|^2}}{\int \mathrm{d}\psi_-(\omega_m)\, \mathrm{d}\psi_-^*(\omega_m)\, e^{-T\,E_-|\psi_-(\omega_m)|^2}}\right. \\
&\qquad\left. \times \frac{\int \mathrm{d}\psi_+(\omega_m)\, \mathrm{d}\psi_+^*(\omega_m)\, e^{-T\,E_+|\psi_+(\omega_m)|^2}}{\int \mathrm{d}\psi_+(\omega_m)\, \mathrm{d}\psi_+^*(\omega_m)\, e^{-T\,E_+|\psi_+(\omega_m)|^2}}\right].
\end{aligned}$$

Thus, the solution of above equation yields

$$\begin{aligned}
\langle|\phi_3(\omega_m)|^2\rangle &= \frac{1}{T}\left[\frac{\sin^2(\theta/2)}{E_+} + \frac{\cos^2(\theta/2)}{E_-}\right] \\
&= \frac{4}{T(4\alpha_2\alpha_3 - J_{23}^2)}\left[\frac{(\alpha_2+\alpha_3)}{2} - \frac{\cos\theta}{2}\sqrt{(\alpha_2-\alpha_3)^2 + J_{23}^2}\right].
\end{aligned}$$

Use of the definition in equation (F.1) simplifies this equation to

$$\left\langle |\phi_3(\omega_m)|^2 \right\rangle = \frac{4\alpha_2}{T(4\alpha_2\alpha_3 - J_{23}^2)} \,. \tag{F.7}$$

Thus, the constraint for $\phi_3(\omega_m)$ is

$$T\sum_{\omega_m} \frac{4\alpha_2}{(4\alpha_2\alpha_3 - J_{23}^2)} = 1 \,,$$

which is

$$\int_0^\infty \frac{(\epsilon_2 + \gamma_2\omega)\mathrm{d}\omega}{(\epsilon_2 + \gamma_2\omega)(\epsilon_3 + \gamma_3\omega) - \frac{J_{23}^2}{4}} = \pi \tag{F.8}$$

at zero temperature. This integral is solved by defining

$$\frac{(\epsilon_2 + \gamma_2\omega)/\gamma_2\gamma_3}{\omega^2 + (\epsilon_2\gamma_3 + \gamma_2\epsilon_3)\omega/\gamma_2\gamma_3 + (4\epsilon_2\epsilon_3 - J_{23}^2)/4\gamma_2\gamma_3} = \frac{A'}{B'+\omega} + \frac{C'}{D'+\omega}$$

such that

$$\begin{aligned} A' + C' &= \frac{1}{\gamma_3} \quad , \quad A'D' + B'C' = \frac{\epsilon_2}{\gamma_2\gamma_3} \\ B'D' &= \frac{4\epsilon_2\epsilon_3 - J_{23}^2}{4\gamma_2\gamma_3} \quad , \quad B' + D' = \frac{\epsilon_2}{\gamma_2} + \frac{\epsilon_3}{\gamma_3} \,. \end{aligned} \tag{F.9}$$

Thus,

$$\begin{aligned} B' = B &= \frac{1}{2}\left(\frac{\epsilon_2}{\gamma_2} + \frac{\epsilon_3}{\gamma_3}\right) + \frac{1}{2}\sqrt{\left(\frac{\epsilon_2}{\gamma_2} - \frac{\epsilon_3}{\gamma_3}\right)^2 + \frac{J_{23}^2}{\gamma_2\gamma_3}}, \\ D' = D &= \frac{4\epsilon_2\epsilon_3 - J_{23}^2}{4\gamma_2\gamma_3 B}, \\ A' &= \frac{B\gamma_2 - \epsilon_2}{\gamma_2\gamma_3(B-D)} \quad , \quad C' = \frac{\epsilon_2 - \gamma_2 D}{\gamma_2\gamma_3(B-D)} \,. \end{aligned} \tag{F.10}$$

Therefore, the integral in equation (F.8) is

$$\int_0^\Lambda \frac{A'}{B+\omega}\,\mathrm{d}\omega + \int_0^\Lambda \frac{C'}{D+\omega}\,\mathrm{d}\omega = \pi \,.$$

The solution of this equation is

$$A' \ln\left(\frac{B+\Lambda}{B}\right) + C' \ln\left(\frac{D+\Lambda}{D}\right) = \pi \ .$$

Because Λ is much greater than B and D, this equation can be reduced to

$$A'\gamma_3 \ln\left(\frac{D}{B}\right) + \ln\left(\frac{\Lambda}{D}\right) = \pi\gamma_3 \ , \tag{F.11}$$

where the definition of $A'+C'$ in (F.9) is used. Thus, this equation gives the constraint for site 3.

The sum of the constraints at sites 2 and 3 (i.e., equations (F.6) and (F.11) respectively) gives

$$\pi(\gamma_2+\gamma_3) = 2\ln\Lambda + (A\gamma_2 + A'\gamma_3 - 2)\ln D - (A\gamma_2 + A'\gamma_3)\ln B \ .$$

The use of definitions of A, A' and $B+D$ in equations (F.5), (F.10), and (F.4) respectively modifies the above equation to

$$\pi(\gamma_2+\gamma_3) = \ln\frac{\Lambda^2}{BD} \ .$$

Thus, the effective distance from the critical point (i.e., equation (65)) in terms of damping coefficients at sites 2 and 3, and in terms of cut-off frequency is

$$2\frac{\epsilon_2\epsilon_3 - J_{23}^2/4}{J_{23}} = 2\frac{\gamma_2\gamma_3\Lambda^2 e^{-\pi(\gamma_2+\gamma_3)}}{J_{23}} \ , \tag{F.12}$$

in which BD is defined as in equation (F.4).

APPENDIX G

DISTANCE FROM THE CRITICAL POINT OF A TWO-SITE CLUSTER FOR SUPEROHMIC DAMPING

The thermal average of $\phi_2(\omega_m)$ yields the constraint at site 2. Thus, for the functional S defined in equation (99), it is

$$\langle|\phi_2(\omega_m)|^2\rangle = \frac{\int |\phi_2(\omega_m)|^2 \, \mathrm{d}\phi_2(\omega_n) \, \mathrm{d}\phi_2^*(\omega_n) \, \mathrm{d}\phi_3(\omega_n) \, \mathrm{d}\phi_3^*(\omega_n) \, e^{-S}}{\int \mathrm{d}\phi_2(\omega_n) \, \mathrm{d}\phi_2^*(\omega_n) \, \mathrm{d}\phi_3(\omega_n) \, \mathrm{d}\phi_3^*(\omega_n) \, e^{-S}}.$$

Equation (101) yields this average in eigenbasis ψ_+ and ψ_-:

$$\frac{\int \mathrm{D}[\psi_+\psi_-](\omega_n) \, (\cos^2(\theta/2)|\psi_+(\omega_m)|^2 + \sin^2(\theta/2)|\psi_-(\omega_m)|^2) \, e^{-S'}}{\int \mathrm{D}[\psi_+\psi_-](\omega_n) \, e^{-S'}}$$

with S' as defined in equation (102). For a frequency ω_m, this equation is reduced to

$$\frac{\int \mathrm{D}[\psi_+\psi_-](\omega_m)[\cos^2(\theta/2)|\psi_+(\omega_m)|^2 + \sin^2(\theta/2)|\psi_-(\omega_m)|^2] \, e^{-S_{\omega_m}}}{\int \mathrm{D}[\psi_+\psi_-](\omega_m) \, e^{-S_{\omega_m}}}$$
$$\times \frac{\int \mathrm{D}[\psi_+\psi_-](\omega_{n\neq m}) \, e^{-S'}}{\int \mathrm{D}[\psi_+\psi_-](\omega_{n\neq m}) \, e^{-S'}}$$

with $S_{\omega_m} = T(E_+|\psi_+(\omega_m)|^2 + E_-|\psi_-(\omega_m)|^2)$. The solution of the first term is obtained by using equation (C.3), which expresses the thermal average as

$$\begin{aligned}\langle|\phi_2(\omega_m)|^2\rangle &= \frac{1}{T}\left[\frac{\sin^2(\theta/2)}{E_-} + \frac{\cos^2(\theta/2)}{E_+}\right] \\ &= \frac{4}{T(4\alpha_2\alpha_3 - J_{23}^2)}\left[\frac{(\alpha_2+\alpha_3)}{2} + \frac{\cos\theta}{2}\sqrt{(\alpha_2-\alpha_3)^2 + J_{23}^2}\right],\end{aligned}$$

where α_2 is equal to $\epsilon_2 + \gamma_2|\omega_n|^{2/z_0}$ and α_3 is equal to $\epsilon_3 + \gamma_3|\omega_n|^{2/z_0}$, and

$$\cos\theta = \frac{\alpha_3 - \alpha_2}{\sqrt{(\alpha_2-\alpha_3)^2 + J_{23}^2}}. \tag{G.1}$$

Thus,

$$\langle|\phi_2(\omega_m)|^2\rangle = \frac{4\alpha_3}{T(4\alpha_2\alpha_3 - J_{23}^2)}. \tag{G.2}$$

Therefore, the constraint at site $\phi_2(\omega_m)$ is

$$T\sum_{\omega_m} \frac{4\alpha_3}{(4\alpha_2\alpha_3 - J_{23}^2)} = 1.$$

At absolute zero, this equation becomes an integral:

$$\int_0^\infty \frac{(\epsilon_2 + \gamma_2\omega^{2/z_0})\mathrm{d}\omega}{(\epsilon_2 + \gamma_2\omega^{2/z_0})(\epsilon_3 + \gamma_3\omega^{2/z_0}) - \frac{J_{23}^2}{4}} = \pi \ . \tag{G.3}$$

This equation is solved by defining

$$\frac{(\epsilon_3 + \gamma_3\omega^y)/\gamma_2\gamma_3}{\omega^{2y} + (\epsilon_2\gamma_3 + \gamma_2\epsilon_3)\omega^y/\gamma_2\gamma_3 + (4\epsilon_2\epsilon_3 - J_{23}^2)/4\gamma_2\gamma_3} = \frac{A}{B+\omega^y} + \frac{C}{D+\omega^y} \ ,$$

where y is equal to $2/z_0$. The variables A, B, C, and D are similar to those defined in equation (F.5) in the ohmic case above. Thus, equation (G.3) is reduced to

$$\int_0^\infty \frac{A}{B+\omega^y}\,\mathrm{d}\omega + \int_0^\infty \frac{C}{D+\omega^y}\mathrm{d}\omega = \pi \ .$$

The definition $\omega^y = Bx^y$ expresses the first integral above as

$$AB^z \int_0^\infty \frac{\mathrm{d}x}{1+x^y} \ ,$$

where z is equal to $1/y - 1$. In this expression, the integral is a constant c_1. A similar technique is used to solve the second integral, which yields the constraint at site 2 (i.e., equation (G.3)):

$$c_1 AB^z + c_2 CD^z = \pi \ . \tag{G.4}$$

The effective distance from the critical point $\tilde{\epsilon}$ is derived below using this equation, along with the constraint at site 3. That constraint is derived using the thermal average of $\phi_3(\omega_m)$, which is

$$\frac{\int \mathrm{D}[\psi_+\psi_-](\omega_m)\,(\sin^2(\theta/2)|\psi_+(\omega_m)|^2 + \cos^2(\theta/2)|\psi_-(\omega_m)|^2)\,e^{-S'}}{\int \mathrm{D}[\psi_+\psi_-](\omega_m)\,e^{-S'}}$$

in the eigenbasis ψ_+ and ψ_-. The steps outlined above for calculation of the constraint

at site 2 yield

$$\langle|\phi_3(\omega_m)|^2\rangle = \frac{1}{T}\left[\frac{\cos^2(\theta/2)}{E_-} + \frac{\sin^2(\theta/2)}{E_+}\right]$$
$$= \frac{4}{T(4\alpha_2\alpha_3 - J_{23}^2)}\left[\frac{(\alpha_2+\alpha_3)}{2} - \frac{\cos\theta}{2}\sqrt{(\alpha_2-\alpha_3)^2 + J_{23}^2}\right] .$$

Thus,

$$\langle|\phi_3(\omega_m)|^2\rangle = \frac{4\alpha_2}{T(4\alpha_2\alpha_3 - J_{23}^2)} , \tag{G.5}$$

which uses equation (G.1). Hence,

$$T\sum_{\omega_m}\frac{4\alpha_2}{(4\alpha_2\alpha_3 - J_{23}^2)} = 1 ,$$

which is the constraint for $\phi_3(\omega_m)$. At absolute zero, this equation is reduced to

$$\int_0^\infty \frac{(\epsilon_2 + \gamma_2\omega^{2/z_0})\mathrm{d}\omega}{(\epsilon_2 + \gamma_2\omega^{2/z_0})(\epsilon_3 + \gamma_3\omega^{2/z_0}) - \frac{J_{23}^2}{4}} = \pi . \tag{G.6}$$

Equation (G.6) is solved by defining

$$\frac{(\epsilon_2 + \gamma_2\omega^y)/\gamma_2\gamma_3}{\omega^{2y} + (\epsilon_2\gamma_3 + \gamma_2\epsilon_3)\omega^y/\gamma_2\gamma_3 + (4\epsilon_2\epsilon_3 - J_{23}^2)/4\gamma_2\gamma_3} = \frac{A'}{B'+\omega^y} + \frac{C'}{D'+\omega^y} ,$$

where y is equal to $2/z_0$. The variables A', B', C', and D' are as defined above in equation (F.10) for the ohmic case. The steps outlined above to calculate the integrals for site 2 yield the constraint at site 3 (i.e., equation (G.6)):

$$c_1A'B^z + c_2C'D^z = \pi . \tag{G.7}$$

Definition of C in equation (F.4) and C' in equation (F.9) expresses equations (G.4) and (G.7) as

$$\gamma_2A(c_1B^z - c_2D^z) + c_2D^z = \pi\gamma_2 \text{ and}$$
$$\gamma_3A'(c_1B^z - c_2D^z) + c_2D^z = \pi\gamma_3$$

respectively. The sum of these two equations is

$$\pi(\gamma_2+\gamma_3) = (\ln b - \ln d)(\gamma_2 A + \gamma_3 A') + 2\ln d\,,$$

where $\ln b$ is equal to $c_1 B^z$ and $\ln d$ is equal to $c_2 D^z$. Use of definition of A and A', given in equations (F.5) and (F.10) respectively, expresses this equation as

$$\pi(\gamma_2+\gamma_3) = \frac{2(B\ln b - D\ln d)}{B-D} + \left(\frac{\gamma_2\epsilon_3+\epsilon_2\gamma_3}{\gamma_2\gamma_3(B-D)}\right)\ln\left(\frac{d}{b}\right)\,.$$

The definition of $B+D$ in equation (F.4) reduces this equation to

$$\pi(\gamma_2+\gamma_3) = \frac{2(B\ln b - D\ln d)}{B-D} + \left(\frac{B+D}{B-D}\right)\ln\left(\frac{d}{b}\right)\,,$$

which can be further simplified as

$$\pi(\gamma_2+\gamma_3) = c_1 B^{\frac{z_0}{2}-1} + c_2 D^{\frac{z_0}{2}-1}\,. \tag{G.8}$$

This equation is solved using the definitions of B and $B+D$ in equations (F.5) and (F.4) respectively. The following redefines B as

$$B = \frac{1}{2}\left[\frac{X_2+J_{23}/2}{\gamma_2} + \frac{X_3+J_{23}/2}{\gamma_3} + \left(\frac{(X_2+J_{23}/2)^2}{\gamma_2^2} + \frac{(X_3+J_{23}/2)^2}{\gamma_3^2} - \frac{2(X_2+J_{23}/2)(X_3+J_{23}/2)+J_{23}^2}{\gamma_2\gamma_3}\right)^{1/2}\right]\,,$$

where the substitutions $\epsilon_2 = X_2 + J_{23}/2$ and $\epsilon_3 = X_3 + J_{23}/2$ are used. This equation can be simplified as

$$B = \frac{1}{2}\left[\left(\frac{X_2}{\gamma_2}+\frac{X_3}{\gamma_3}+\frac{J_{23}}{2}\left(\frac{1}{\gamma_2}+\frac{1}{\gamma_3}\right)\right) + \left(\left(\frac{X_2}{\gamma_2}-\frac{X_3}{\gamma_3}\right)^2 + J_{23}\left(\frac{X_2}{\gamma_2^2}+\frac{X_3}{\gamma_3^2}-\frac{X_2+X_3}{\gamma_2\gamma_3}\right) + \frac{J_{23}^2}{4}\left(\frac{1}{\gamma_2}+\frac{1}{\gamma_3}\right)^2\right)^{1/2}\right]\,.$$

The term $\left(\frac{X_2}{\gamma_2}-\frac{X_3}{\gamma_3}\right)^2$ is discarded because it is small. Thus, this equation is reduced

to

$$B = \frac{1}{2}\left[\left(\frac{X_2}{\gamma_2} + \frac{X_3}{\gamma_3} + \frac{J_{23}}{2}\left(\frac{1}{\gamma_2} + \frac{1}{\gamma_3}\right)\right) - \frac{J_{23}}{2}\left(\frac{1}{\gamma_2} + \frac{1}{\gamma_3}\right)\left(1 + \frac{4\left(\frac{X_2}{\gamma_2^2} + \frac{X_3}{\gamma_3^2} - \frac{X_2+X_3}{\gamma_2\gamma_3}\right)}{J_{23}\left(\frac{1}{\gamma_2} + \frac{1}{\gamma_3}\right)}\right)^{1/2}\right] .$$

The expansion of the square root term yields

$$B = \frac{1}{2}\left[\frac{X_2}{\gamma_2} + \frac{X_3}{\gamma_3} - \frac{X_2\gamma_3}{\gamma_2(\gamma_2+\gamma_3)} - \frac{X_3\gamma_2}{\gamma_3(\gamma_2+\gamma_3)} + \frac{X_2+X_3}{(\gamma_2+\gamma_3)}\right] .$$

Thus,

$$B = \frac{X_2 + X_3}{\gamma_2 + \gamma_3} . \tag{G.9}$$

Similarly, D is equal to

$$\frac{1}{2}\left[\left(\frac{\epsilon_2}{\gamma_2} + \frac{\epsilon_3}{\gamma_3}\right) - \sqrt{\left(\frac{\epsilon_2}{\gamma_2} - \frac{\epsilon_3}{\gamma_3}\right)^2 + \frac{J_{23}^2}{\gamma_2\gamma_3}}\right] ,$$

which uses the definition of $B + D$ in equation (F.4) and B in equation (F.5). The steps outlined above in the simplification of B express D as

$$D = \frac{X_2 + X_3}{\gamma_2 + \gamma_3} . \tag{G.10}$$

Thus, equations (G.9) and (G.10) express equation (G.8) as

$$c\pi(\gamma_2 + \gamma_3)^{z_0/2} = (X_2 + X_3)^{z_0/2-1} . \tag{G.11}$$

BIBLIOGRAPHY

[1] Ma, S. K. *Modern Theory Of Critical Phenomenon.* Benjamin, (1976).

[2] Stanley, H. E. *Introduction To Phase Transitions and Critical Phenomena.* Oxford University Press, (1971).

[3] Papon, P., Lablond, J., and Meijer, P. *The Physics Of Phase Transitions.* Springer, (2002).

[4] Binney, J. J., Dowrick, N. J., Fisher, A. J., and Newman, M. E. J. *The Theory Of Critical Phenomena- An Introduction To The Renormalization Group.* Oxford University Press, (1998).

[5] Andrews, T. *Phil. Trans. R. Soc.* **159**, 575 (1869).

[6] Bally, D., Grabchev, B., Popovici, M., Totia, M., and Lungu, A. M. *J. Appl. Phys.* **39**, 459 (1968).

[7] Collins, M. F., Minkiewicz, V. J., Natans, R., Passell, L., and Shirane, G. *Phys. Rev.* **179**, 417 (1969).

[8] Rocker, E., Kohlhaus, R., and Schopgens, A. W. *Z. Agnew. Phys.* **32**, 164 (1971).

[9] Heller, P. *Rep. Prg. Phys.* **30**, 731 (1967).

[10] Widom, B. *J. Chem. Phys.* **45**, 3892 (1965).

[11] Wilson, K. G. and Kogut, J. *Phys. Rep.* **12**, 75 (1974).

[12] Pathria, R. K. *Statistical Mechanics.* Elsevier, (2004).

[13] Chaikin, P. and Lubensky, T. *Principles Of Condensed Matter Physics.* Cambridge University Press, (2003).

[14] Herbut, I. *A Modern Approach To Critical Phenomena.* Cambridge University Press, (2007).

[15] Vojta, T. *Ann. Phys.* **9**, 403 (2000).

[16] Vojta, M. *Rep. Prg. Phys.* **66**, 2069 (2003).

[17] Sachdev, S. *Quantum Phase Transitions.* Cambridge University Press, (1999).

[18] Bitko, D., Rosenbaum, T. F., and Aeppli, G. *Phys. Rev. Lett.* **77**, 940 (1996).

[19] Trotter, H. F. *Proc. Am. Math. Soc.* **10**, 545 (1959).

[20] Suzuki, M. *Commun. Math. Phys.* **51**, 183 (1976).

[21] Harris, A. B. *J. Phys. C: Solid State Phys.* **7**, 1671 (1974).

[22] Vojta, T. *J. Phys. A: Math. Gen.* **39**, R143 (2006).

[23] Griffiths, R. B. *Phys. Rev. Lett.* **23**, 17 (1969).

[24] Randeria, M., Sethan, J., and Palmer, R. G. *Phy. Rev. Lett.* **54**, 1321 (1985).

[25] Landau, L. D. *Phys. Z. Sowjetunion* **11**, 26 (1937).

[26] Landau, L. D. *Zh. Eksp. Teor. Fiz.* **7**, 19 (1937).

[27] Landau, L. D. *Zh. Eksp. Teor. Fiz.* **7**, 627 (1937).

[28] Landau, L. D. *Phys. Z. Sowjetunion* **11**, 545 (1937).

[29] ter Harr, D., editor. *Collected Papers Of L. D. Landau.* Gorden and Breach, New York, (1965).

[30] Ginzburg, V. L. *Sov. Phys. Sol. Sta.* **2**, 1824 (1960).

[31] Levanyuk, A. P. *Sov. Phys. JETP* **36**, 571 (1959).

[32] Hubbard, J. *Phys. Rev. Lett.* **3**, 77 (1959).

[33] Stratanovich, R. L. *Sov. Phys. Dokl* **2**, 416 (1958).

[34] Igloi, F. and Monthus, C. *Phys. Rep.* **412**, 277 (2005).

[35] Ma, S. K., Dasgupta, C., and Hu, C. K. *Phys. Rev. Lett.* **43**, 1434 (1979).

[36] Dasgupta, C. and Ma, S. K. *Phys. Rev. B* **22**, 1305 (1980).

[37] Goldenfeld, N. *Lectures On Phase Transitions And The Renormalization Group.* Westview Press, (1992).

[38] Zinn-Justin, J. *Quantum Field Theory And Critical Phenomena.* Oxford University Press, (1989).

[39] Amit, D. J. *Field Theory, The Renormalization Group, And Critical Phenomena.* World Scientific, (1984).

[40] Fisher, D. *Phys. Rev. Lett.* **69**, 534 (1992).

[41] Fisher, D. *Phys. Rev. B* **51**, 6411 (1995).

[42] Stewart, G. *Rev. Mod. Phys.* **73**, 797 (2001).

[43] Stewart, G. *Rev. Mod. Phys.* **78**, 743 (2006).

[44] Sereni, J. G., Westerkamp, T., Kuchler, R., Caroca-Canales, N., Gegenwart, P., and Geibel, C. *Phys. Rev. B* **75**, 24432 (2007).

[45] Westerkamp, T., Deppe, M., Kuchler, R., Brando, M., Geibel, C., Gegenwart, P., and Pikul, A. P. *Phys. Rev. Lett.* **102**, 206404 (2009).

[46] Ubaid-Kassis, S., Vojta, T., and Schroeder, A. *Phys. Rev. Lett.* **104**, 066402 (2010).

[47] Bezryadin, A., Lau, C. N., and Tinkham, M. *Nature* **404**, 971 (2000).

[48] Rogachev, A. and Bezryadin, A. *Appl. Phy. Lett.* **83**, 512 (2003).

[49] Philips, P. *Advanced Solid State Physics.* Westview Press, (2003).

[50] Duan, F. and Guojun, J. *Introduction To Condensed Matter Physics.* World scientific, (2005).

[51] Hewson, A. C. *The Kondo Problem To Heavy Fermions.* Cambridge University Press, (1997).

[52] Anderson, P. *Phys. Rev.* **124**, 41 (1961).

[53] Hubbard, J. *Proc. Roy. Soc. Lond. A* **276**, 238 (1964).

[54] Kim, D. J. *New Perspectives in Magnetism of Metals.* Kluwer academic/ Plenum publisher, (1999).

[55] Gegenwart, P., Si, Q., and Steglich, F. *Nature Physics* **4**, 186 (2008).

[56] Lohneyson, H. V., Rosch, A., Vojta, M., and Wolfel, P. *Rev. Mod. Phys.* **79**, 1015 (2007).

[57] Hertz, J. *Phys. Rev. B* **14**, 1165 (1976).

[58] Millis, A. J. *Phys. Rev. B* **48**, 1993 (1993).

[59] Kirkpatrick, T. R. and Belitz, D. *Phys. Rev. Lett.* **76**, 2571 (1996).

[60] Negele, J. and Orland, H. *Quantum Many-Particle Systems.* Perseus Books,Reading, MA, (1998).

[61] Vojta, T., Belitz, D., Narayanan, R., and Kirkpatrick, T. R. *Z. Phys. B* **103**, 451 (1996).

[62] Belitz, D., Kirkpatrick, T. R., and Vojta, T. *Rev. Mod. Phys.* **77**, 579 (2005).

[63] Belitz, D., Kirkpatrick, T. R., and Vojta, T. *Phys. Rev. B* **55**, 9452 (1997).

[64] Stoner, E. C. *Rep. Prg. Phys.* **11**, 43 (1947).

[65] Hoyos, J. A., Kotabage, C., and Vojta, T. *Phys. Rev. Lett.* **99**, 230601 (2007).

[66] Vojta, T., Kotabage, C., and Hoyos, J. A. *Phys. Rev. B* **79**, 24401 (2009).

[67] Vojta, T. and Schmalian, J. *Phy. Rev. B* **72**, 45438 (2005).

[68] Vojta, T., Hoyos, J. A., Mohan, P., and Narayanan, R. *arXiv:1008.1106v1* (2010).

[69] Altman, E., Kafri, Y., Polkovnikov, A., and Refael, G. *Phy. Rev. Lett.* **93**, 150402 (2004).

[70] Vojta, T. *Phy. Rev. Lett.* **90**, 107202 (2003).

[71] Maestro, A. D., Rosenow, B., and Sachdev, S. *Ann. Phys. (N.Y.)* **324**, 523 (2009).

[72] Sachdev, S., Werner, P., and Troyer, M. *Phys. Rev. Lett.* **92**, 237003 (2004).

[73] Maestro, A. D., Rosenbow, B., Shah, N., and Sachdev, S. *Phy. Rev. B* **77**, 180501(R) (2008).

VITA

Chetan Vyankatesh Kotabage was born in Wai, Maharashtra, India on October 12, 1975. He received his B.Sc. degree in Physics with first class in May 1997 from University of Pune, Pune, Maharashtra, India. He received his M.Sc. in Physics with second class in December 2000 from University of Pune, Pune, Maharashtra, India. He earned his M. Tech. (Master of Technology) degree in Opto-electronics and Laser technology with distinction from Cochin University of Science and Technology, Cochin, Kerala, India in June 2004.